Long-term variations of the galactic cosmic rays dose rates

T. Dachev[1], P. Dimitrov[1], B. Tomov[1], Y. Matviichuk[1], J. Semkova[1]
R. Koleva[1], M. Jordanova[1], N. Bankov[1], V. Shurshakov[2], V. Benghin[2]

[1]Space Research & Technology Institute, Bulgarian Academy of Sciences, Sofia, 1113, Bulgaria, tdachev59@gmail.com

[2]Institute of Medical and Biological Problems, Russian Academy of Sciences, Moscow, Russia

Outlook

- Introduction
- Liulin instruments description
- Data selection procedures
- Long-term variations of the measured by Liulin instruments GCR dose rates
  - Altitudinal dependence in the dose rate
  - Global (latitudinal) dependence in the dose rate
  - Shielding dependence in the dose rate
- Comparison of Liulin GCR dose measurements with other experiments and models
- Conclusions

Introduction

Scientific objectives of the 14 Liulin experiments?

1. Measurement of the variations of the flux and dose rate from GCR, SCR, IRB and ORB in LEO and in interplanetary space. Use of data in models;

In LEO

On rocket

In interpl. space

6 experiments from 14

2. Support of the biological and chemical experiments with actual information about the history of the dose accumulation. Also radiation variation measurements.

Foton-M2/3, BION-M1, Foton-M4

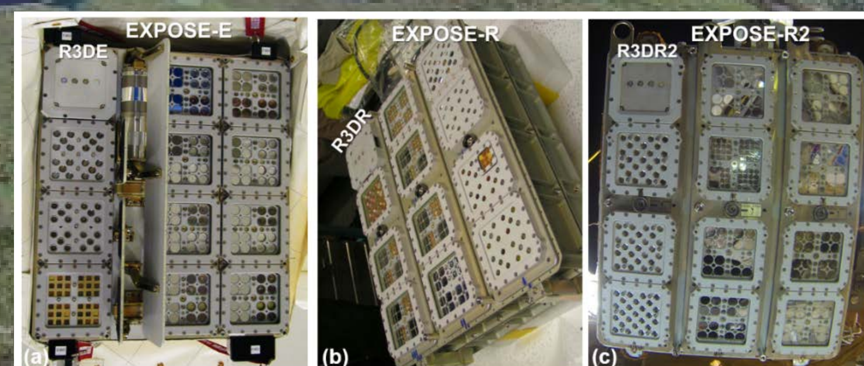

ISS, Expose-E/R/R2

8 experiments from 14

Liulin instruments description

Generalized block diagram of Liulin-type DES instruments

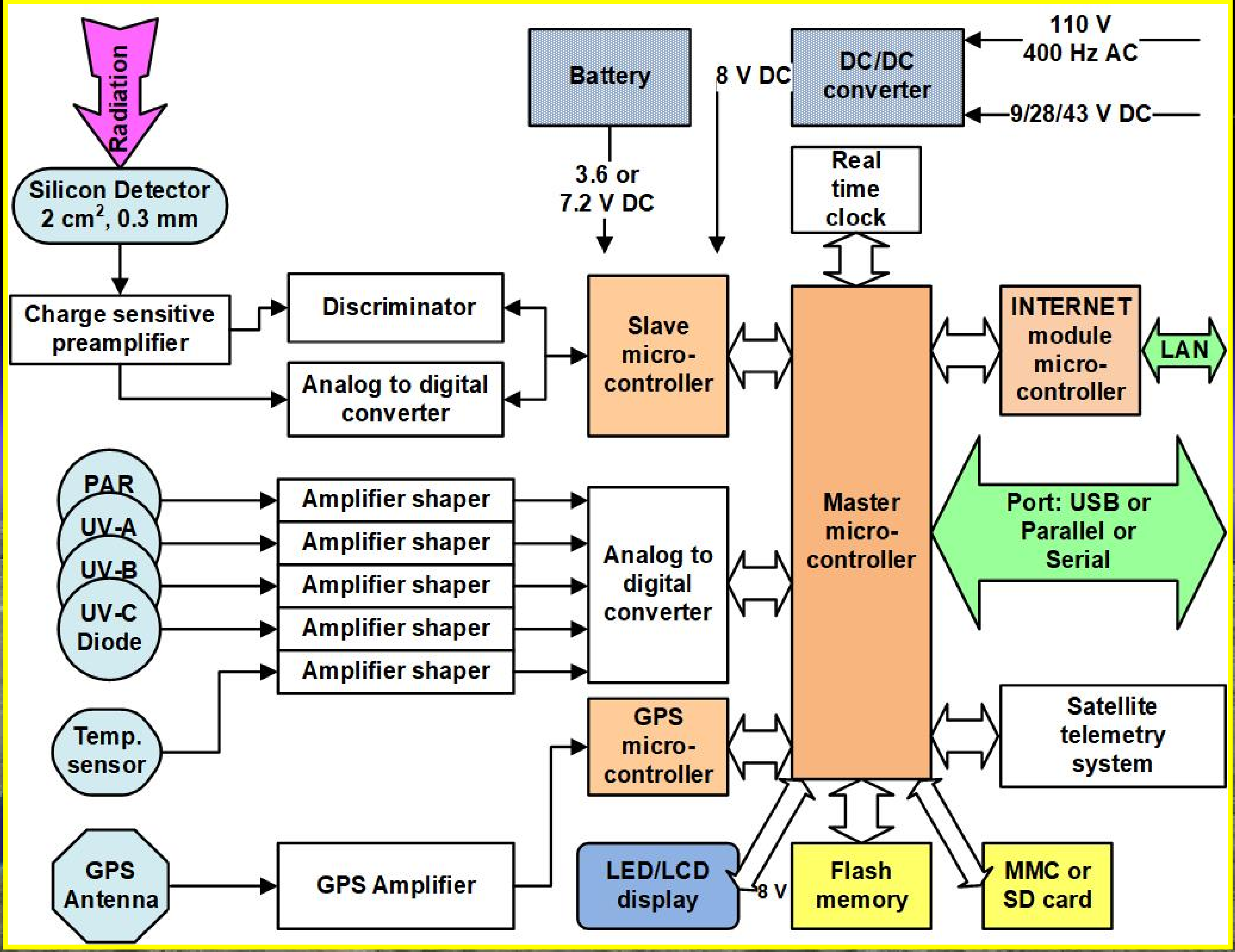

Functional diagram of FREND dosimeter Liulin-MO

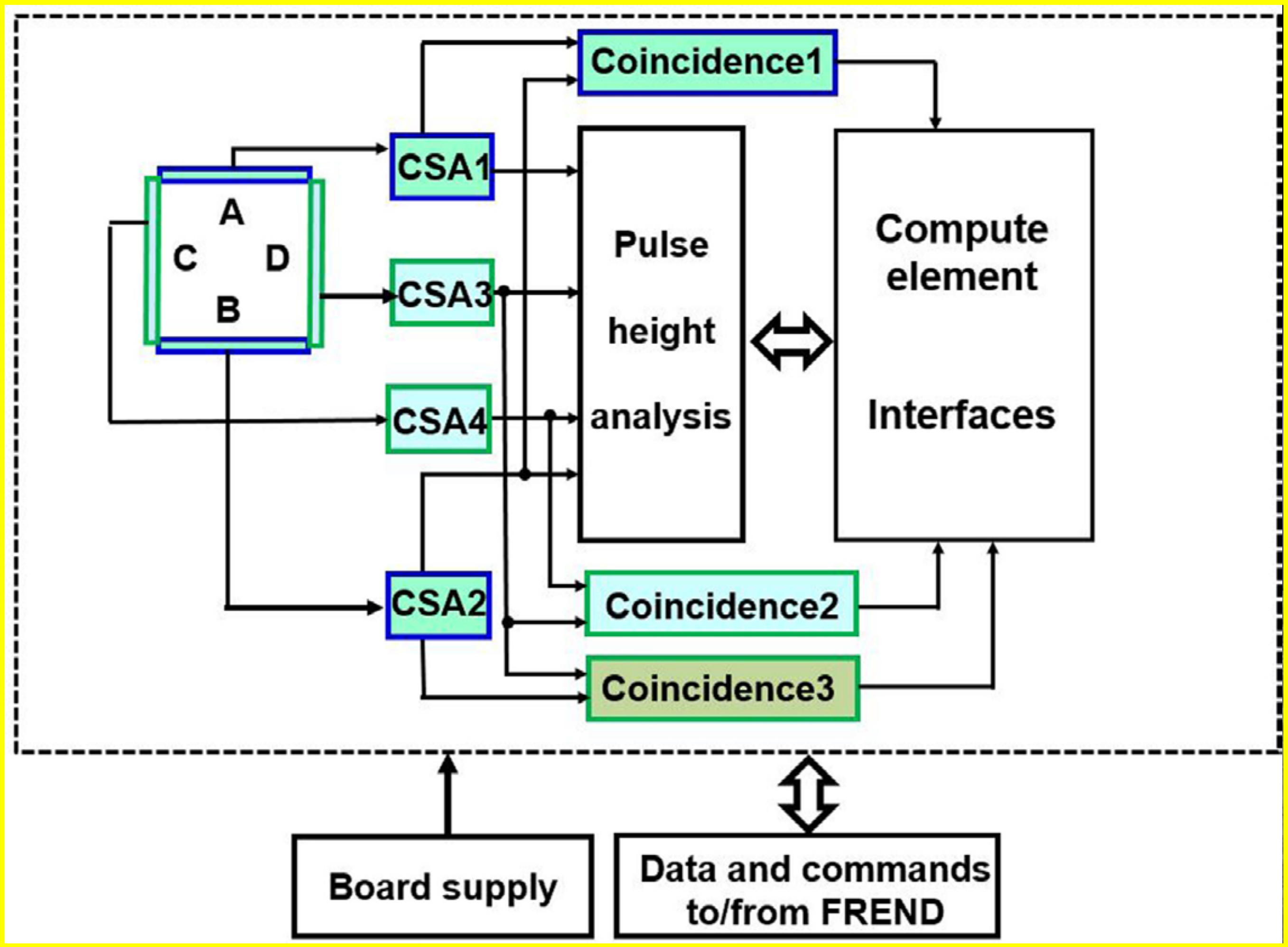

Dose calculation procedure applied in Liulin instrument

By definition the dose in the silicon detector D_{Si} [Gy] is one joule deposited in 1 kg of matter. The LTK absorbed dose is calculated by dividing the summarized energy deposition in the spectrum in joules by the mass of the detector in kilograms:

$$D_{Si}[Gy] = K\sum_{i=1}^{255}(EL_i i)[J]/MD[kg]$$

where K is a coefficient. MD is the mass of the detector, and EL_i is the energy loss in Joules in channel i. The energy in MeV is proportional to the amplitude A of the pulse: $EL_i[MeV]=A[V]/0.24[V/MeV]$, where $0.24[V/MeV]$ is a coefficient dependent on the preamplifier used and its sensitivity.

All 255 deposited dose values, depending on the deposited energy for one exposure period, form the deposited energy spectrum. Channel 256 accumulates all pulses with amplitudes higher than the upper energy of 20.83 MeV measured by the spectrometer.

Source selection procedures

The following four primary radiation sources were expected and recognized in the data obtained with the Liulin instruments:

→ Globally distributed GCR particles and those derived from them;

→ Protons in the SAA region of the inner radiation belt (IRB);

→ Relativistic electrons and/or bremsstrahlung in the high latitudes of the ISS orbit where the outer radiation belt (ORB) is situated;

→ Solar energetic particles (SEP) in the high latitudes of the ISS orbit. Together with the real SEP particles, a low flux of what were likely to be mostly secondary protons (SP) were observed in the data. SEP were observed only in the RD3R2 data.

Dose to Flux (D/F) calculations, based on Haffner formulas*

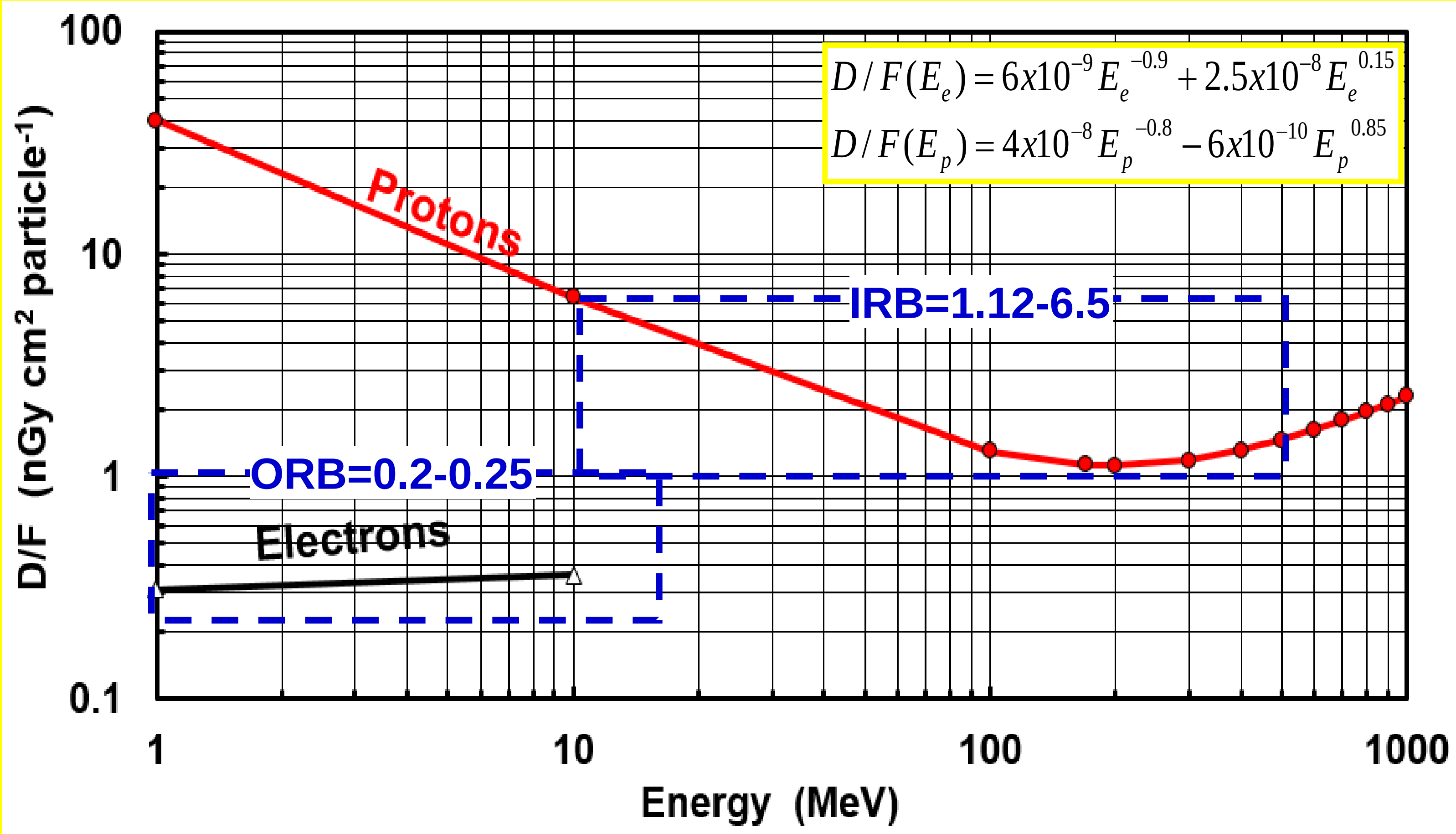

$$D/F(E_e) = 6x10^{-9} E_e^{-0.9} + 2.5x10^{-8} E_e^{0.15}$$

$$D/F(E_p) = 4x10^{-8} E_p^{-0.8} - 6x10^{-10} E_p^{0.85}$$

The valid ranges for D/F(Ee) and D/F(Ep) are 1-10 MeV, and 1-1000 MeV, respectively

Haffner, J.W., Yadernoe izluchenie i zashchita v kosmose (Nuclear Radiation and Protection in Space), pp 115, Atomizdat, Moscow, 1971. (book in Russian).

Example of the selection procedure used with the R3DR2 instrument

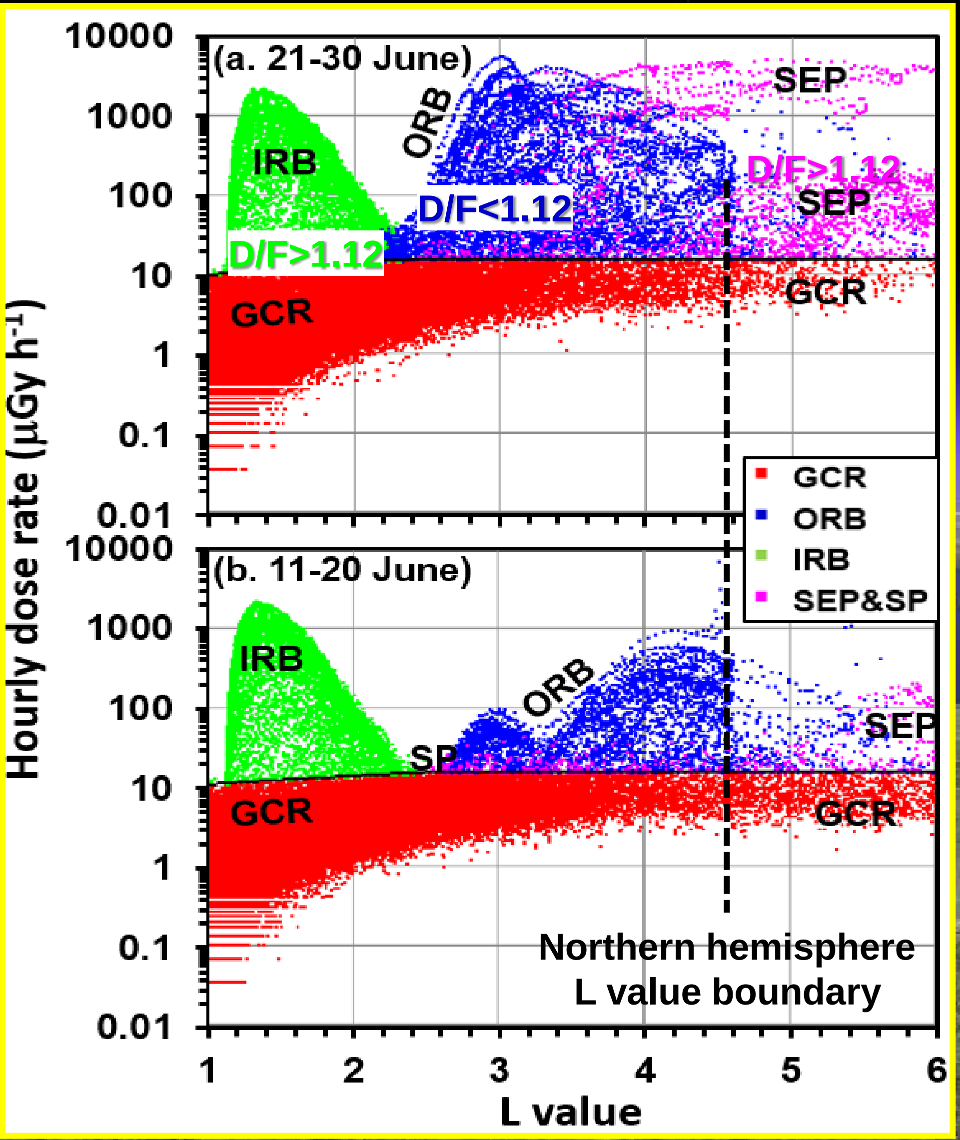

- These 10 days plots were used for the selection of the all 441 days data;

- The selection curve is the black line in the middle of the plots;

- Galactic cosmic rays (GCR) are shown by red points in the lower part of each figure;

- The maximum in the centrum plotted with blue points (ORB) is generated by high-energy electrons;

- The maximum in the upper left corner of the figure plotted by green points (IRB) is created by high-energy protons when the ISS crosses the region of the SAA;

- The magenta points spread from the center toward right side visualize the distribution of the solar high energy protons (SEP&SP).

*Dachev, et al., Space Weather, 15, 1475–1489, 2017.
https://doi.org/10.1002/2016SW001580

Final result of the separation of the R3DR2 instrument data for the period 24 October 2014-11 January 2016 in four radiation sources*

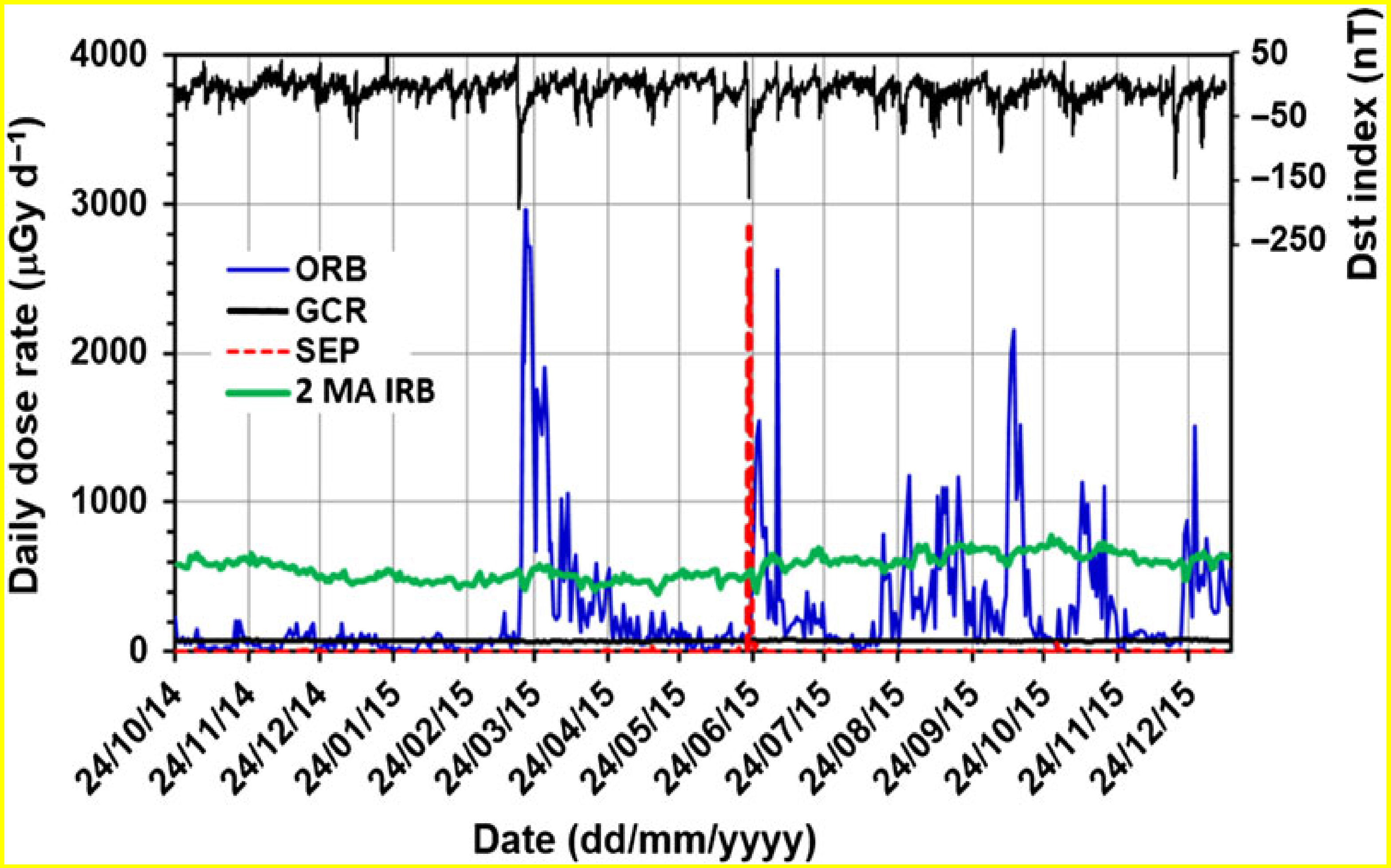

*Dachev, T. P., N. G. Bankov, G. Horneck, D.-P. Häder; Letter to the Editor. Radiat Prot. Dosimetry, 174 (2), 292-295, 2017, https://doi.org/10.1093/rpd/ncw123 .

Long-term variations of the measured by Liulin instruments GCR dose rates

The energy spectra of GCR, measured at Earth, are significantly influenced by the Sun's activity. Traversing the heliosphere, GCRs interact with the expanding solar wind and its embedded turbulent magnetic field, undergoing convection, diffusion, adiabatic energy losses, and particle drifts because of the global curvature and gradients of the heliospheric magnetic field. Therefore, the intensity of GCRs at Earth decreases with respect to the GCR energy spectrum outside the heliosphere. This solar modulation has large effects on low energy cosmic rays (less than a few GeV), while the effects gradually subside as the energy increases, becoming negligible above a few tens of GeV (Strauss & Potgieter, 2014)*

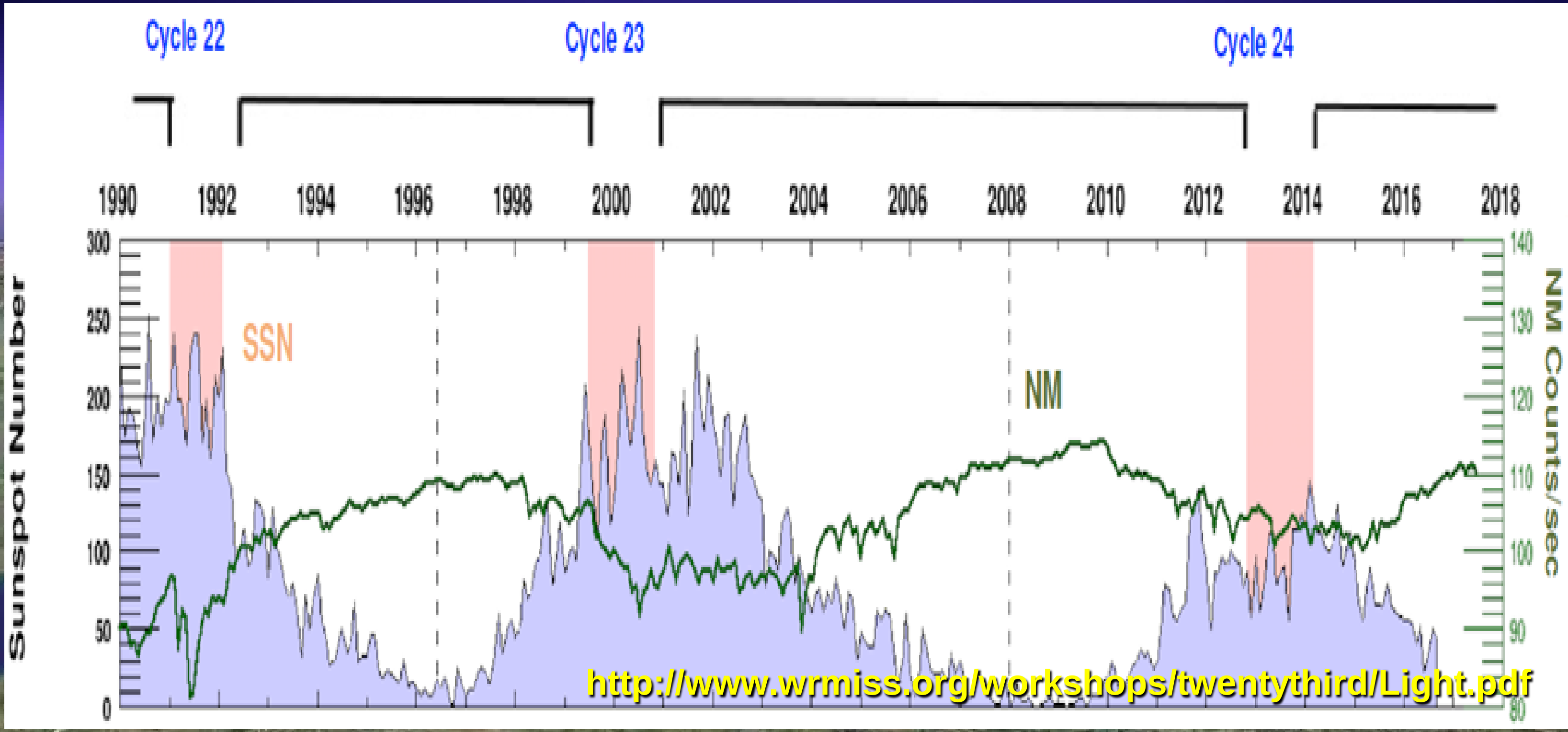

Strauss, R.D. and Potgieter, M.S., 2014. Where does the heliospheric modulation of galactic cosmic rays start?. Advances in Space Research, 53(7), pp.1015-1023. https://doi.org/10.1016/j.asr.2014.01.004

Long-term variations of the averaged flux and dose rates observed in the L rage between 4 and 6.2 during 14 Liulin-type experiments between 2001 and 2019.The Liulin data are compared (red doted line) with the monthly values of the modulation parameter, reconstructed from the ground based cosmic ray data*

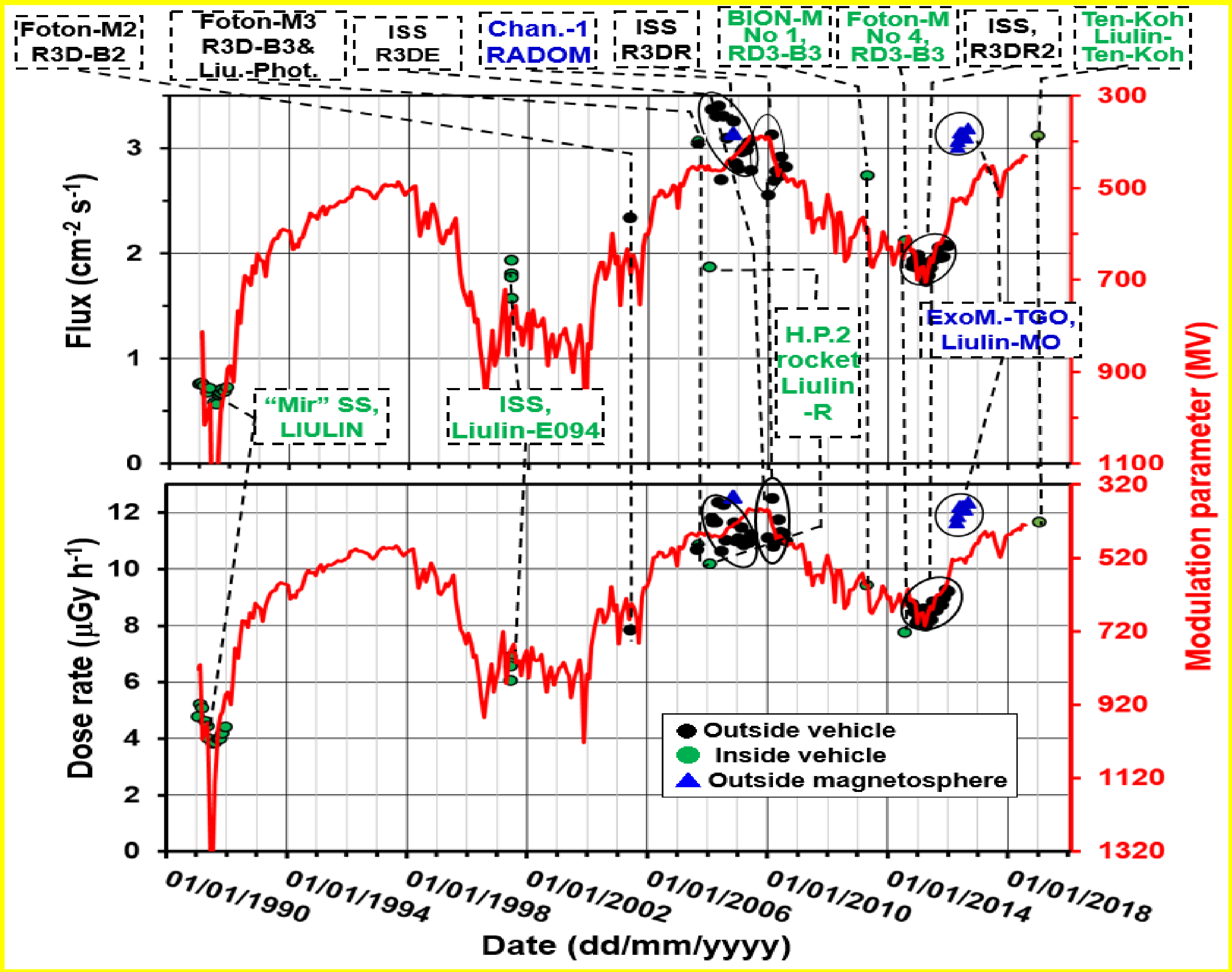

*(Usoskin et al., 2017), http://dx.doi.org/10.1002/2016JA023819

Tabulated data for the 14 Liulin experiments (1)

No	Carrier name, Experiment name, Orbit inclination [Deg], Estimated Shielding [g cm^{-2}]	Time		Number of meas.; Resolut. [sec]; L value	Average characteristics				External view
		Begin (dd/mm/yyyy), Main Reference	End (dd/mm/yyyy)		Altitude Above Earth [km]	Flux [cm^{-2} s^{-1}]	Dose rate [μGy h^{-1}]	D/F ratio [nGy cm^{2} part.$^{-1}$]	
1	Inside "MIR" SS, LIULIN, 51.8°, >20	02/01/1991, (Dachev et al., 1989)	30/12/1991	52,808; 30; >4<6.2	398	0.69	4.37	1.759	
2.1	Inside American segment of ISS, Liulin-E094 (MDU-1), 51.8°, >20	11/05/2001, (Dachev et al., 2002)	25/07/2001	6,411; 30; >4<6.2	403	1.56	6.07	1.070	
2.2	Inside American segment of ISS, Liulin-E094 (MDU-2), 51.8°, >20	11/05/2001, (Dachev et al., 2002)	25/07/2001	6,410; 30; >4<6.2	403	1.84	6.91	1.063	Same as in row 2.1
2.3	Inside American segment of ISS, Liulin-E094 (MDU-3), 51.8°, >20	11/05/2001, (Dachev et al., 2002)	25/07/2001	6,755; 30; >4<6.2	403	1.98	6.67	0.967	Same as in row 2.1
2.4	Inside American segment of ISS, Liulin-E094 (MDU-4), 51.8°, >20	11/05/2001, (Dachev et al., 2002)	25/07/2001	6,755; 30; >4<6.2	403	1.77	6.56	1.028	Same as in row 2.1
3	Outside of Foton-M2 satellite, R3D-B2, 62°, 1.75	01/06/2005, (Häder et al., 2009)	11/06/2005	990; 60; >4<6.2	283	2.34	7.84; 12	0.958	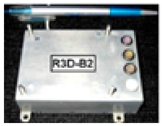
4	Outside of Foton-M3, satellite, R3D-B3, 62°, 0.71	14/09/2007, (Damasso et al., 2009)	26/09/2007	918; 60; >4<6.2	278	3.04	10.70	1.004	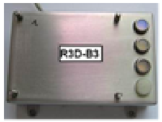
5	Inside of Foton-M3, satellite, Liulin-Photo, 62°, >5	14/09/2007, (Damasso et al., 2009)	26/09/2007	955; 60; >4<6.2	278	2.83	10.82	1.064	

Tabulated data for the 14 Liulin experiments (2)

6	Outside of HotPay2 rocket, Liulin-R, Apogee at 14.04°E, 70.67°N), >20	31/01/2008 (Tomov et al., 2008)	31/01/2008	1; 30; 4.4	377	1.95	10.18	1.452	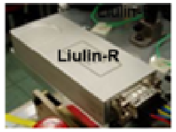
7	Outside of ISS ESA Columbus module, R3DE, 51.8°, 0.3	22/02/2008 (Dachev et al., 2012a)	22/06/2009	107,900; 10; >4<6.2	353	3.23	11.51	1.053	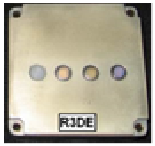
8	Outside of Chandrayaan-1, satellite, RADOM, Moon encounter, 0.45	29/10/2008 (Dachev et al., 2011)	07/11/2008	52,688; 10	230,526	3.08	12.57	1.134	
9	Outside of ISS "Zvezda" module, R3DR, 51.8°, 0.3	20/02/2010, (Dachev et al. 2015)	20/08/2010	27,082; 10; >4<6.2	366	2.89	11.38	1.060	
10	Inside of BION-M No 1, satellite, RD3-B3, 65°, >20	19/04/2013, (Dachev et al. 2014)	13/05/2013	6,442; 60; >4<6.2	567	2.83	9.43	0.955	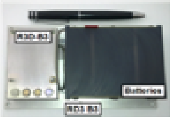
11	Inside of Foton-M No.4, satellite, RD3-B3, 65°, >20	18/07/2014 (Dachev et al. 2015)	31/08/2014	5,998; 60; >4<6.2	399	2.19	7.76	0.969	Same as in row 10
12	ISS, R3DR2, 51.8°, 0.3	25/10/2014, (Dachev et al. 2017)	10/01/2016	322,709, 10; >4<6.2	417	1.9	7.1	1.083	Same as in row 9
13	Outside of ExoMars Trace Gas Orbiter TGO, Liulin-MO, transit to Mars, ~10	22/04/2016, (Semkova et al., 2018)	15/09/2016 (Still operable in Mars orbit)	2164; 3600	75,880,658	3.11	12.08	1.078	
14	Inside of Ten-Koh satellite, Liulin Ten-Koh, 97.8°, ~10	29/10/2018 (Fajardo et al., 2019)	16/01/2019 (Still operable in Earth orbit	12; 29.62; >7	610	2.71	12.68	1.201	

The analysis of Table 1 shows that the 12 experiments in LEO was performed at wide range of shielding from 0.3 up to >20 g cm^2, average altitudes from 278 up to 610 km and globally distributed latitudes and longitudes.

Next part of the presentation is devoted to the dependencies of the GCR dose rate from changes in the, altitude above the Earth, the shielding, and the global latitude and longitude variations.

The objective is to prove that the dose rate value variations caused by the changes in these parameters are less than the variations of the dose rates at L-values higher than 4 induced by the long-term changes in the solar activity.

Altitudinal dependence in the dose rate

Overview of the near Earth radiation environment obtained by RADOM instrument

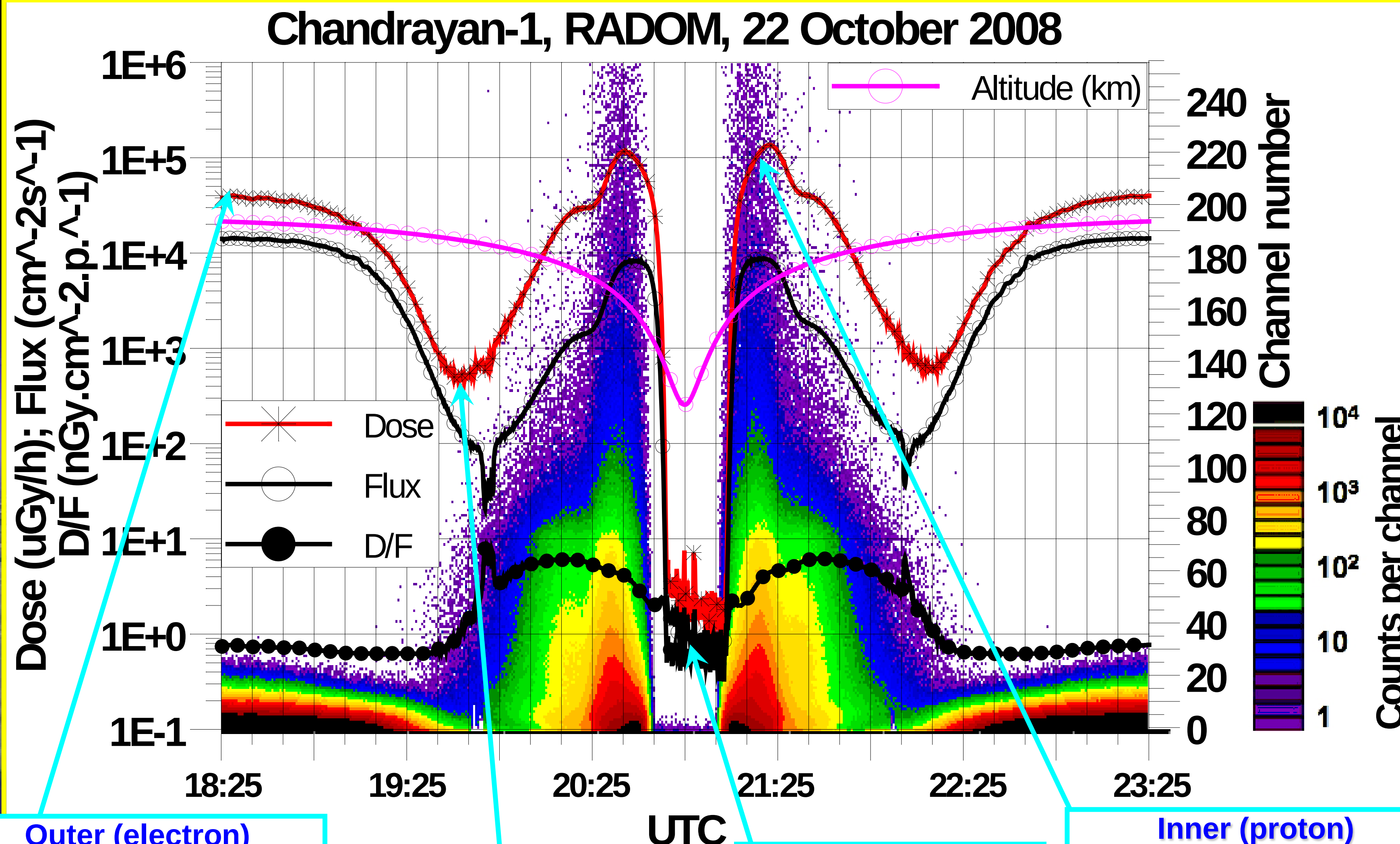

Outer (electron) Radiation belt. Dose = 40000 μGy/h

Slot region Dose = 600 μGy/h

Perigee Dose = 1.2 μGy/h

Inner (proton) radiation belt. Dose = 130000 μGy/h

SRTI, BAS

Experimental altitudinal profile of the dose rate, flux and D/F values, obtained by Liulin instruments

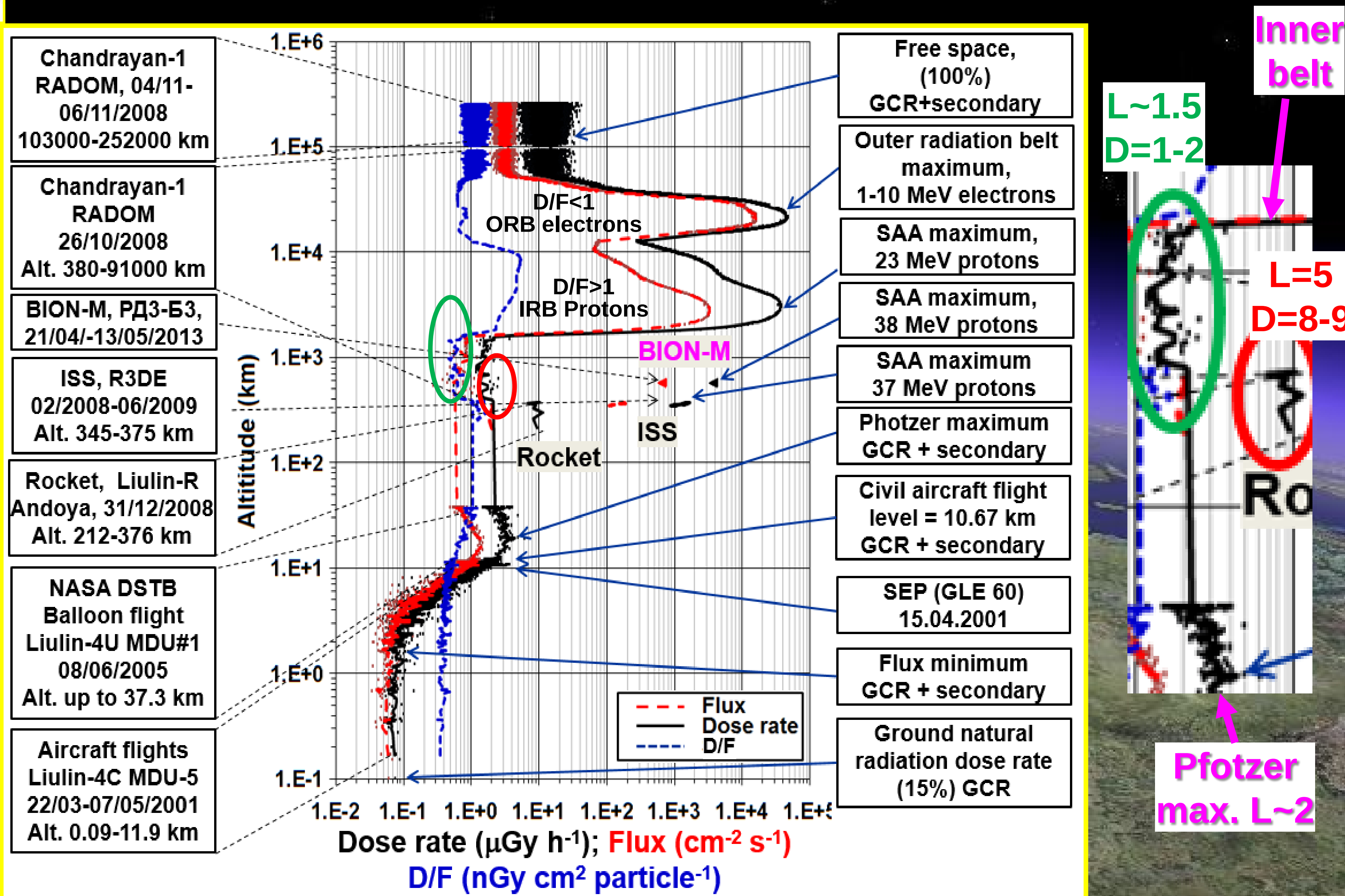

Altitudinal profiles, obtained by the RADOM instrument on the Indian Chandrayaan-1 Moon satellite in low latitudes. Slow rise of the GCR dose rate from 1.5 to 2 μGy h^{-1} is observed in the altitude range from 297 to 1700 km

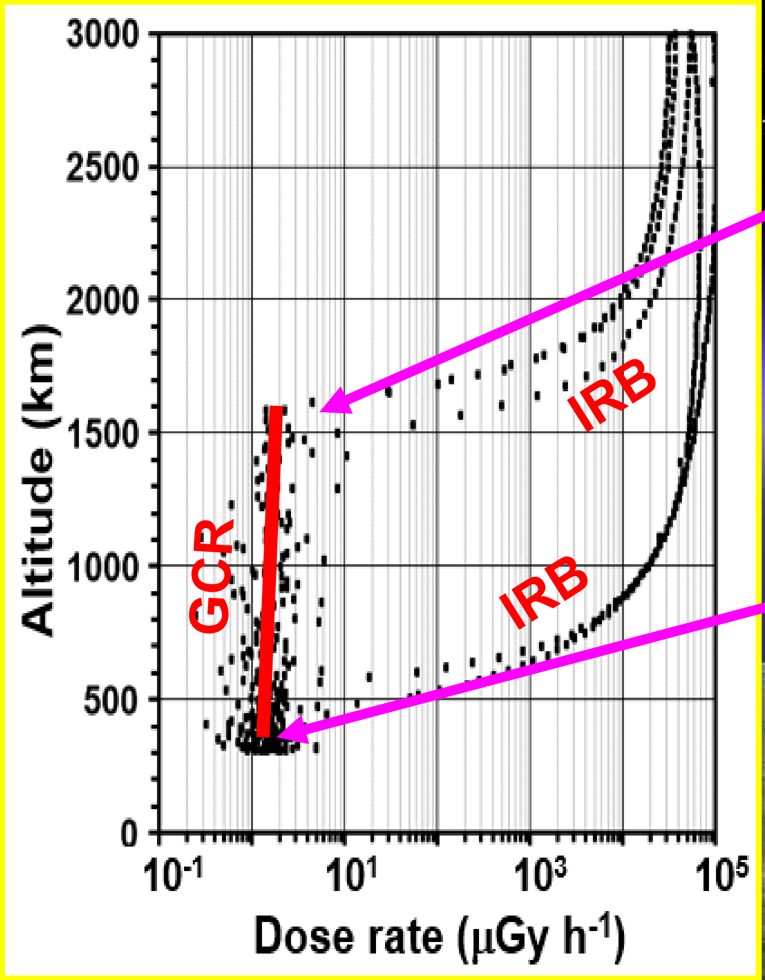

Bottom of the Inner belt out of the region of the SAA~ 1550 km

Bottom of the Inner belt in the region of the SAA ~500 km

Jump in the D/F curve at the altitude of the bottom of IRB

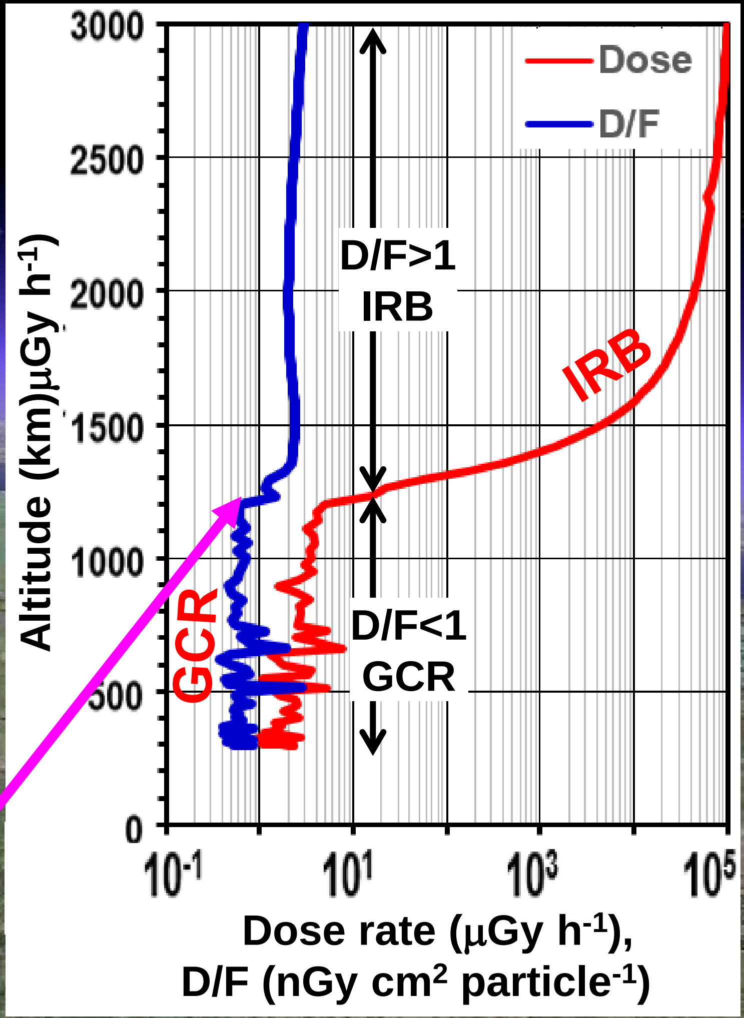

GCR flux, dose rate and D/F altitudinal profiles, obtained by the RD3-B3 instrument on the Foton-M No.4 satellite in L range between 4 and 6.2. Slow rise of the GCR dose rate with altitude from 7 to 8 μGy h^{-1} is observed

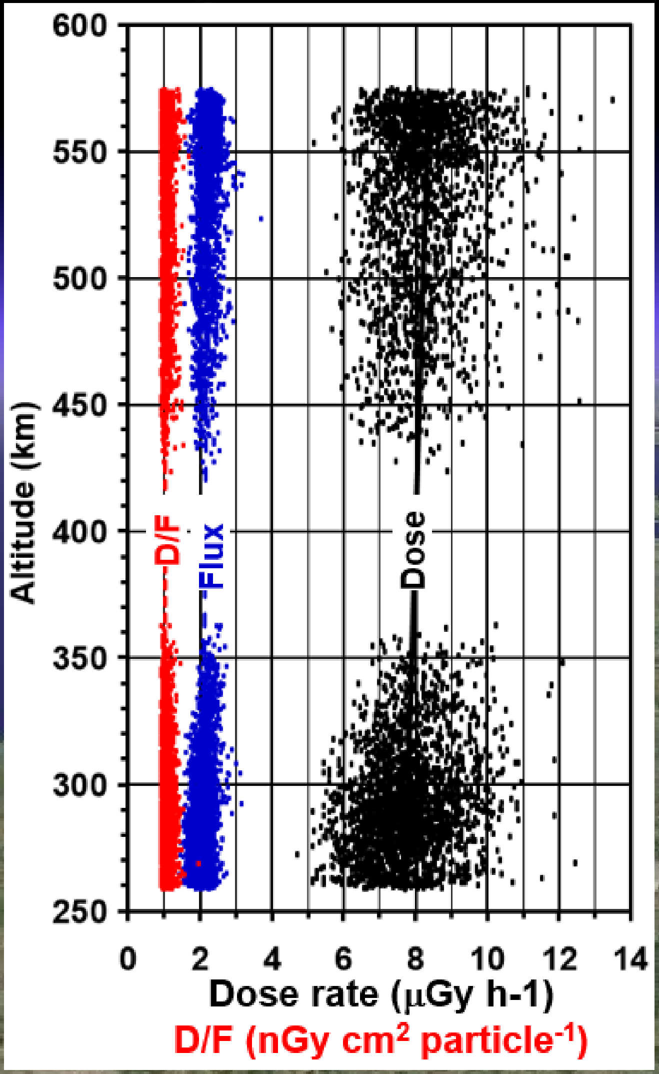

We believe, that the observed above 300 km altitudinal profiles at low and high latitudes are continued down to the altitudes of the Pfotzer maximum as shown by Makhmutov et al., 2016*

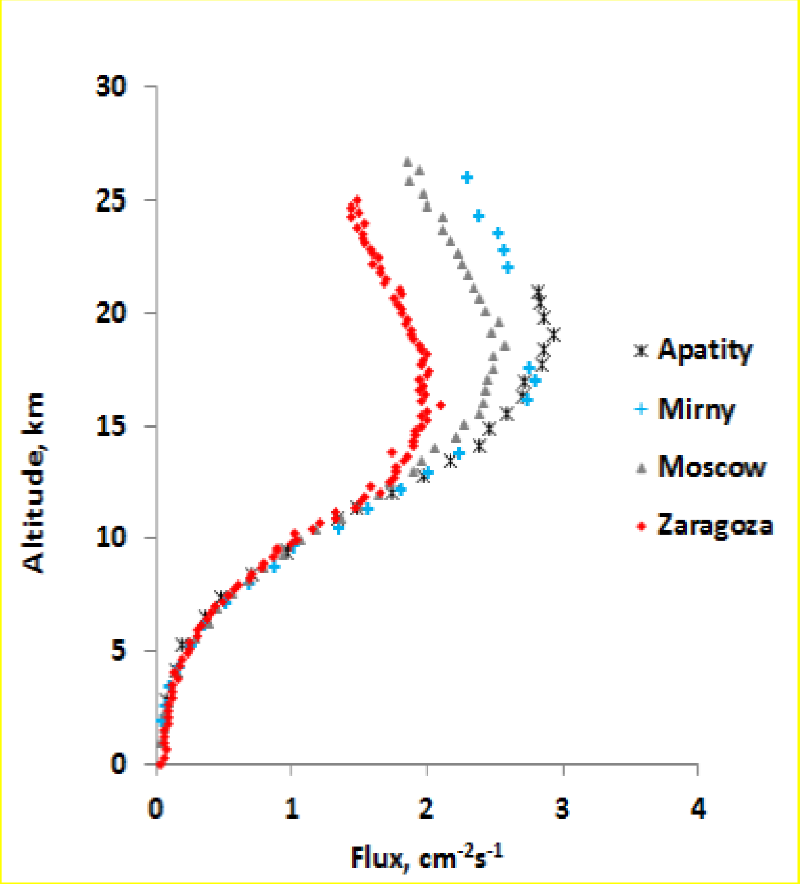

Table 1: Balloon cosmic ray measurements in the atmosphere in October, 2014

Location	Coordinates	Rc(GV)	22.10.2014	24.10.2014
Mirny(Antarctica, RU)	66^o33'S, 93^o00'E	0.03	LPI	LPI
Apatity (RU)	67^o33'N, 33^o24'E	0.56	LPI	LPI
Moscow (RU)	55^o45'N, 37^o37'E	2.36	LPI	LPI
Reading (UK)	51^o27'N, 0^o 58'W	3.6	RDG	
Zaragoza (Spain)	41^o9'N, 0^o54'W	4.6		RDG, LPI
Mitzpe-Ramon (Israel)	30^o36'N, 34^o48'E	10.3	RDG	

*https://www.researchgate.net/publication/298791930_Cosmic_ray_measurements_in_the_atmosphere_at_several_latitudes_in_October_2014

The conclusion from the altitudinal dependence investigation in 350-620 km range is:

The dose rate values in the altitudinal profiles in low and high latitudes are in the range from 1 to 8 $\mu Gy\ h^{-1}$ but the variations in the profile are les than 2 $\mu Gy\ h^{-1}$, which is less than the observed long term variations of 4 to 13 $\mu Gy\ h^{-1}$.

Global (latitudinal) dependence in the dose rate

Global distribution of the dose rate at about 350 km altitude. The map is obtained by averaging of more of 2000 hours ~ 90 days of data. Remarkable is the curve similarity between the lines of equal dose rate and L-value

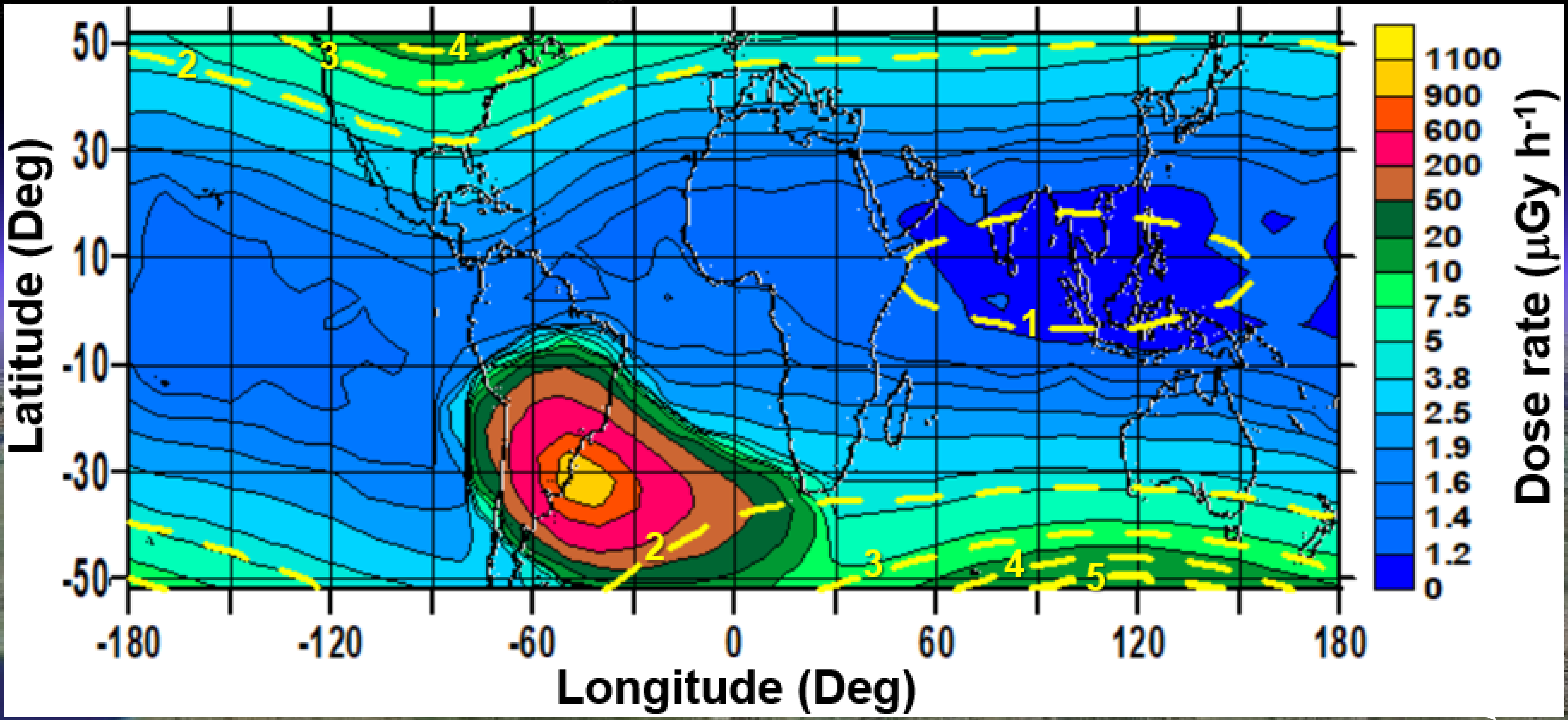

SRTI, BAS

Effective vertical magnetic cutoff rigidities for the 2010 epoch calculated by Smart and Shea using the IGRF 2010 internal reference field for Kp=3; the color bar indicates the notional hazard level based on the increased (lower rigidity) particle flux at higher latitudes (Shea & Smart, 2012)

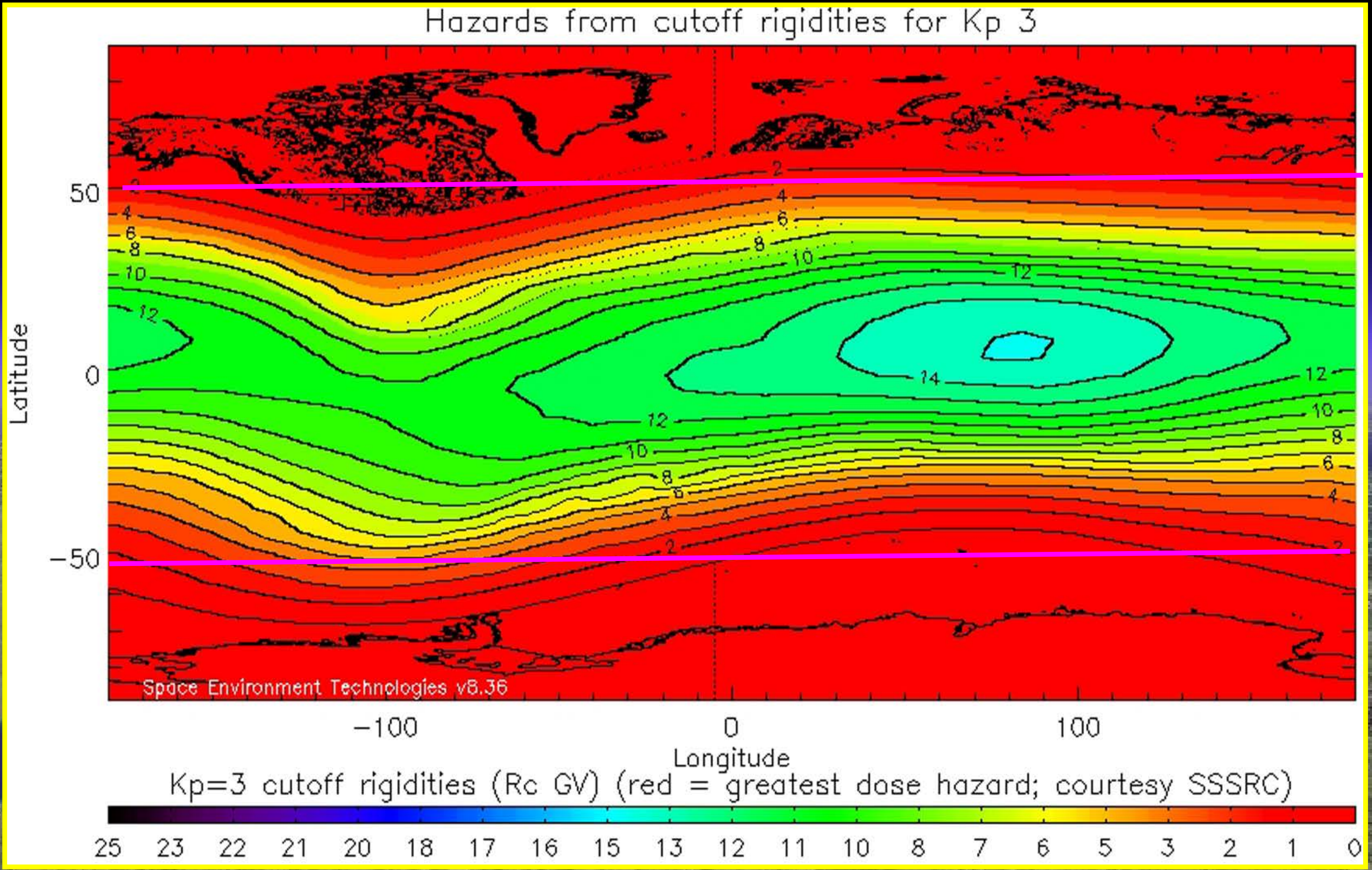

All range L-value profiles of flux, dose rate and D/F data observed between 18 July and 31 August 2014 during the Foton-M No.4 experiment

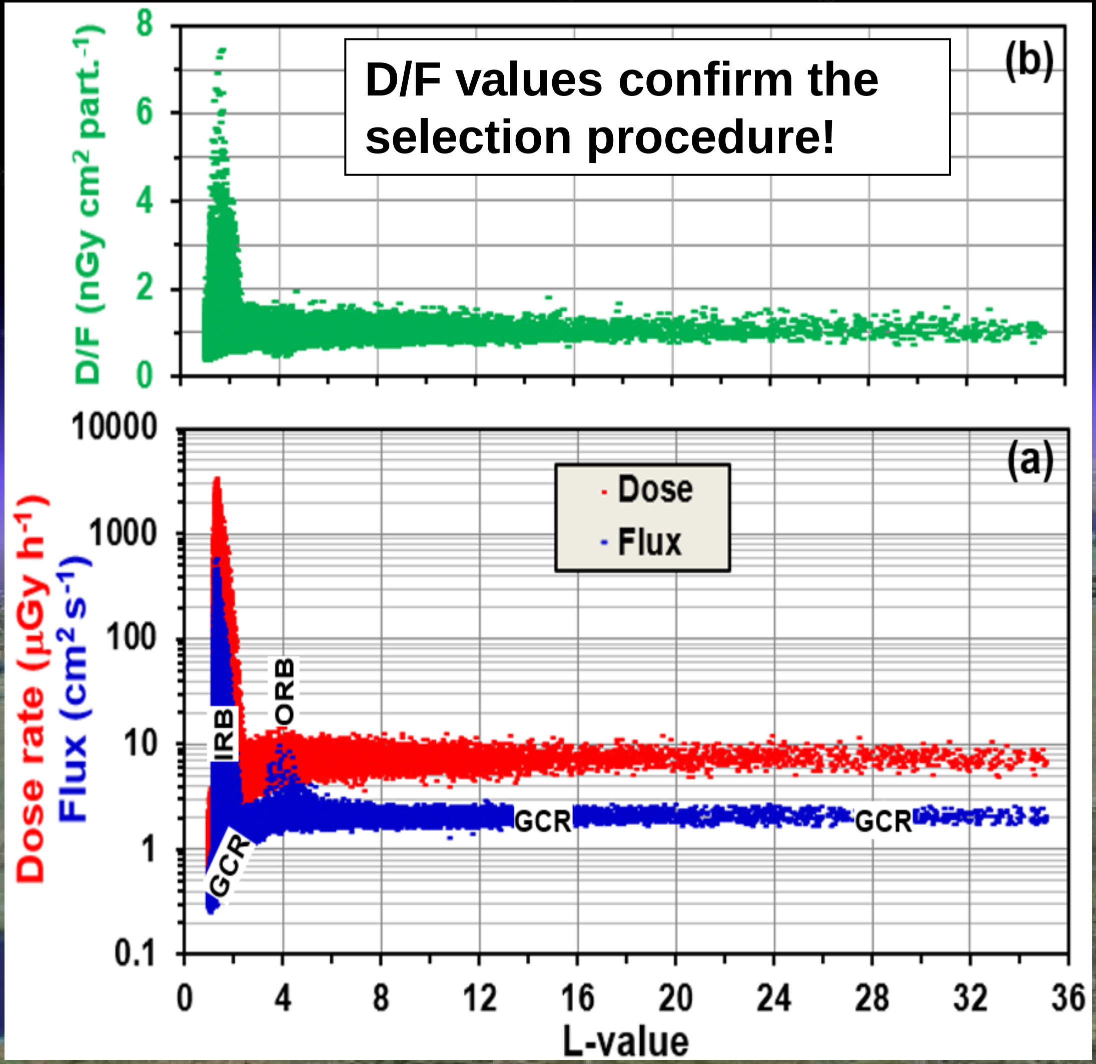

The GCR flux and dose rate data shows minimum in the equatorial region, slow rise toward L=4 and long horizontal tail with equal values toward the maximum L-value of 35.5.

We conclude that:

The GCR doses and fluxes in L range 4<L<6.2 represent adequately the whole L range, which values is close to the free space GCR value.

L-value profiles of the measured dose rate during 5 experiments between 2001 and 2009, which are characterized with decreasing solar activity and respectively increasing GCR dose rates

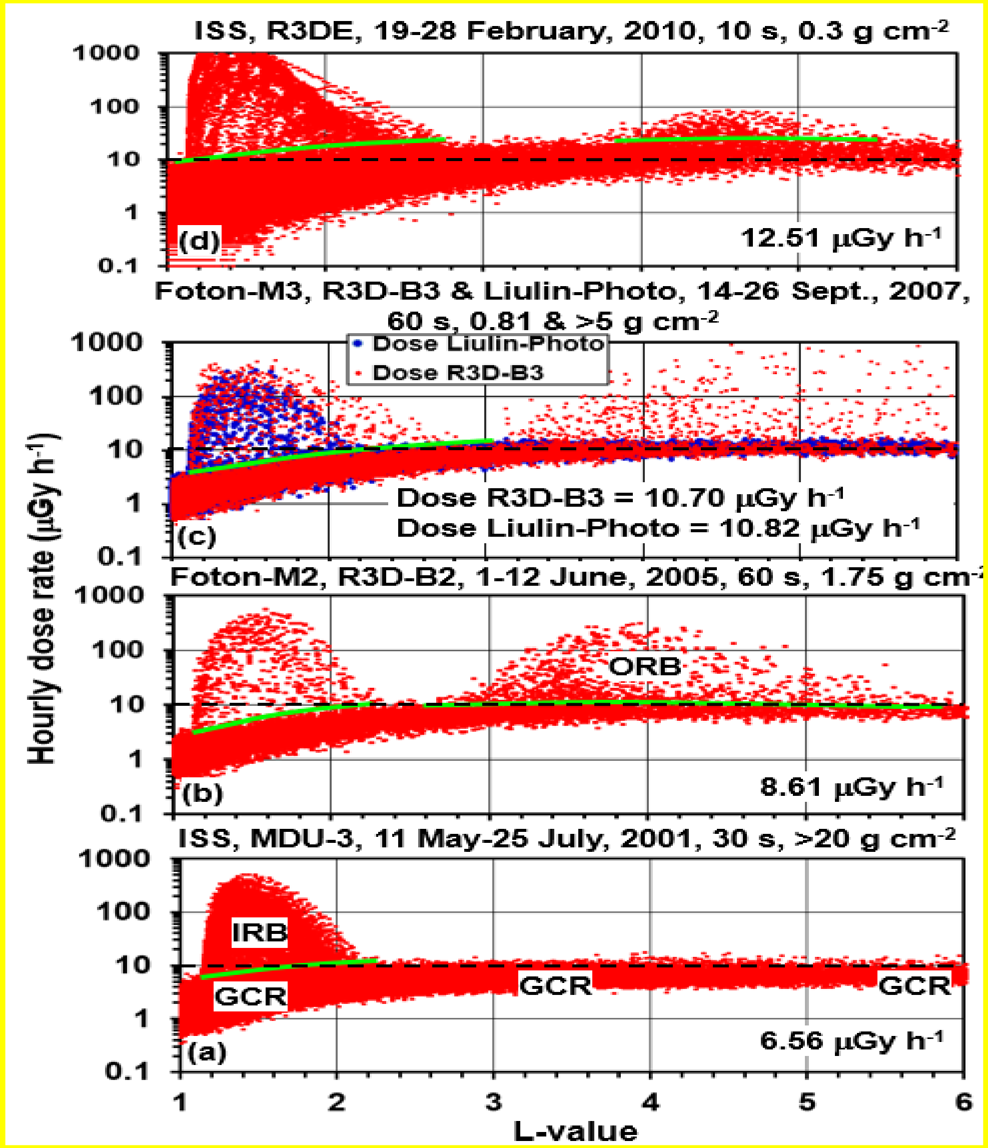

The conclusion from the latitudinal dependence investigation in 350-620 km range is:

Geomagnetic shielding, measured by the vertical cutoff rigidity (Smart & Shea, 2012), is the reason for reduced GCR fluxes and dose rates at low L values in previous slide and the slightly rising dose rate toward L values of 2.5 (Shea et al., 1985). At these increasing L values the vertical cutoff rigidity decreases, and the major amount of the low-energy GCR spectra penetrate down to the ISS orbit. At higher L values, up to L=35, the dose rate has a fixed value because the small increase of the high-energy flux of the primary GCR flux do not affect it. This value is close to the free space value.

The observed average dose rate values from 2001 to 2010 rise from 6.56 to 12.51 $\mu Gy\ h^{-1}$ and confirm the findings in the picture with all 14 experiments.

Shielding dependence in the dose rate

The more shielded by surrounding constructions R3DE instrument measure larger GCR doses than the R3DR instrument

3.83-3.54
=0.29 $\mu Gy\ h^{-1}$

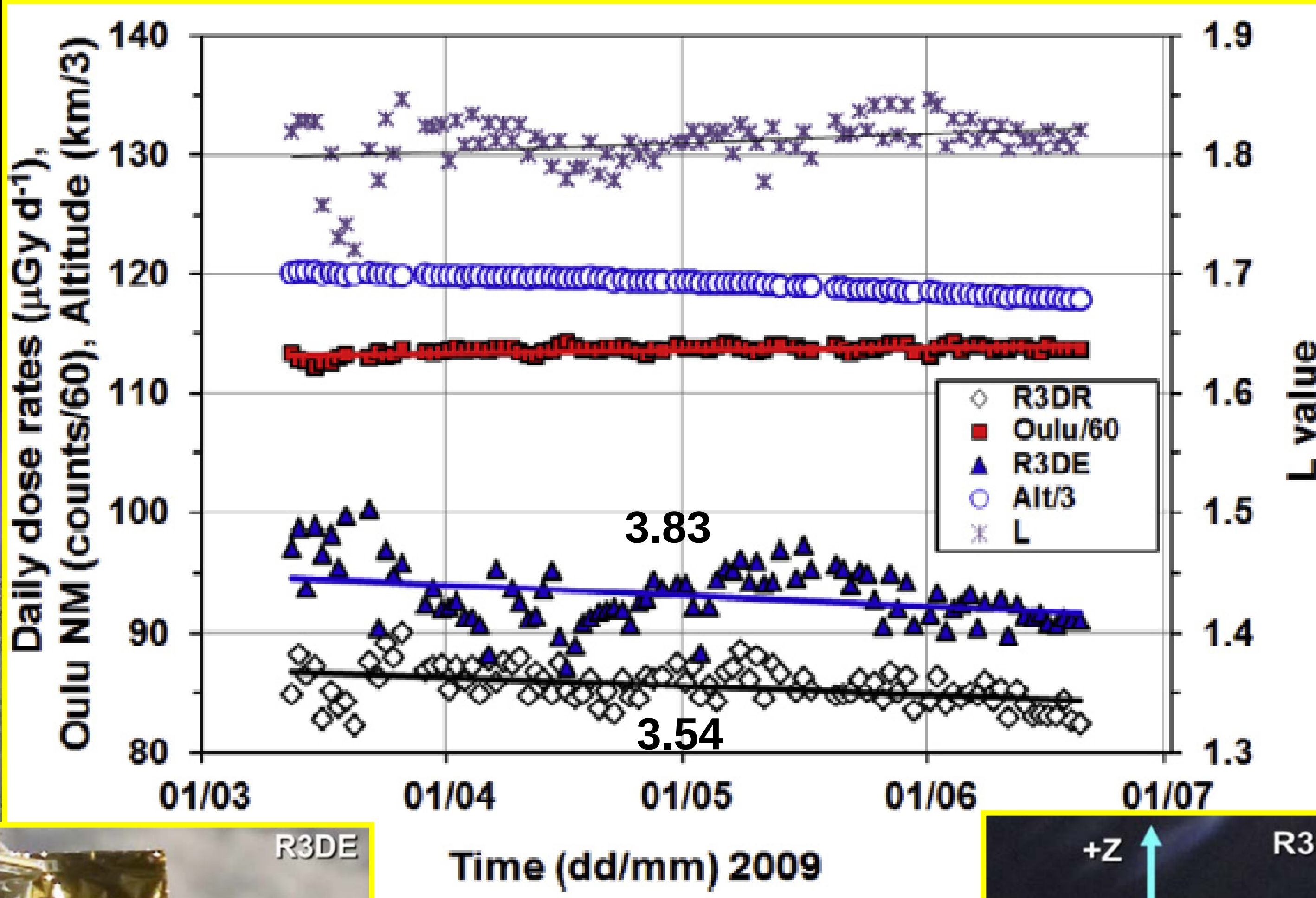

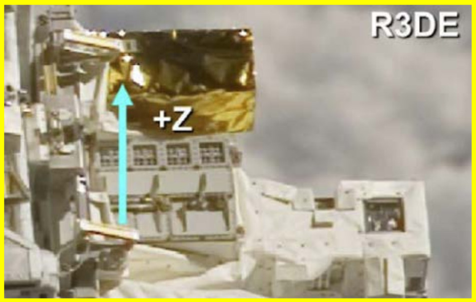

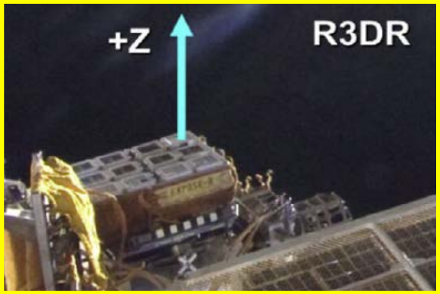

Less shielded R3D-B3 instrument dose rates in the SAA region are larger and extends to larger L-values, while the Liulin-Photo averaged GCR dose rates are higher in the 4<L<6

10.82-10.7 =0.12 μGy h^{-1}

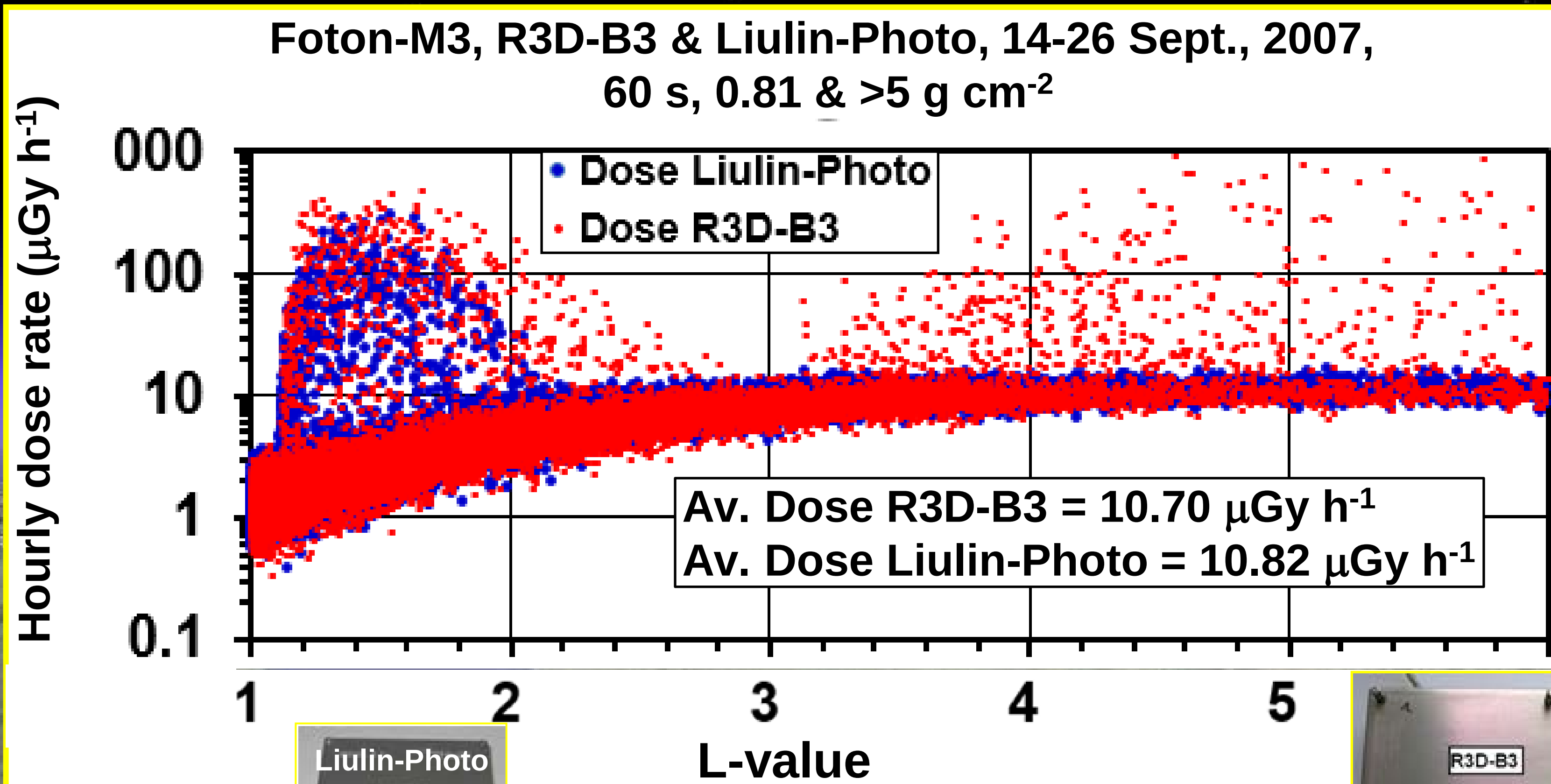

Inside of the satellite
>5 g cm^{-2} shielding

Outside of the satellite
0.71 g cm^{-2} shielding

The GCR dose and flux for L>10 are higher when lid is closed, because the secondary's and neutrons produced in the lid

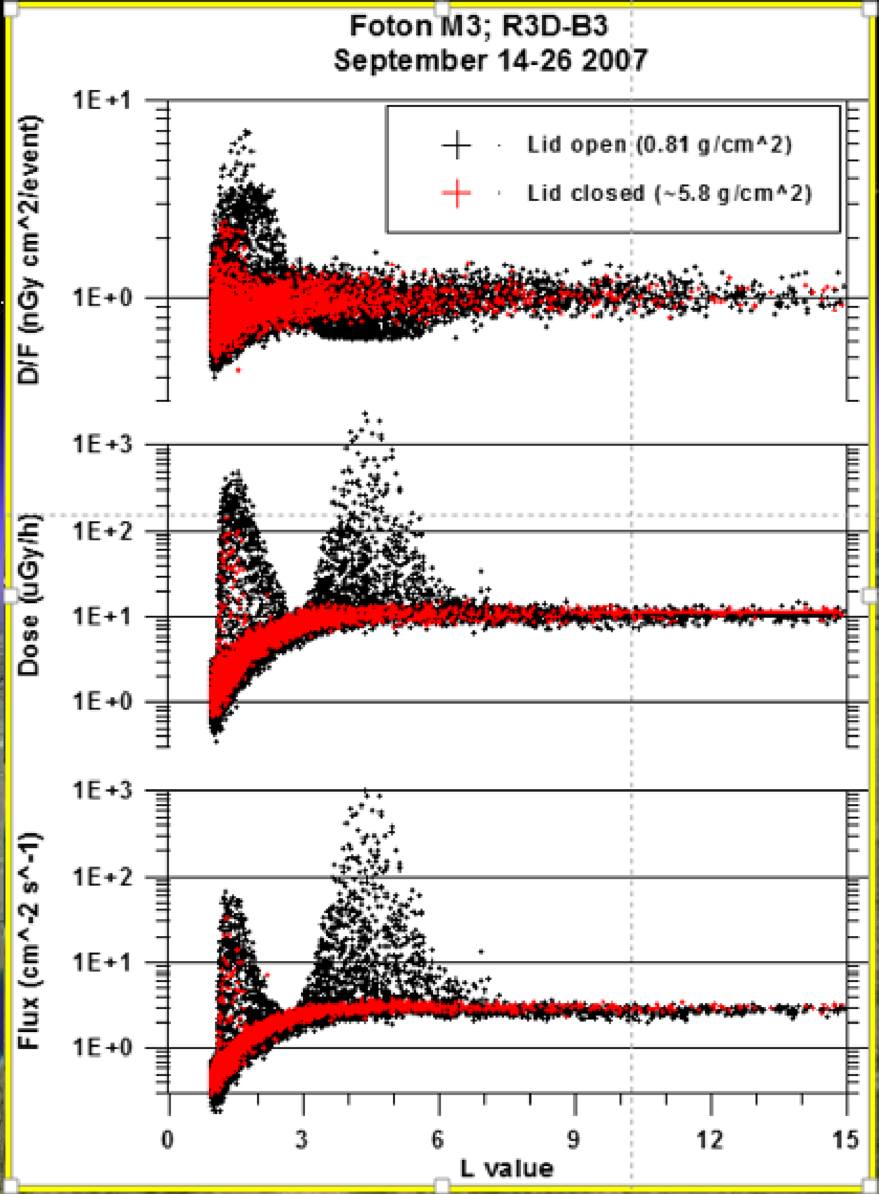

11.12-11.04 =0.08 μGy h^{-1}

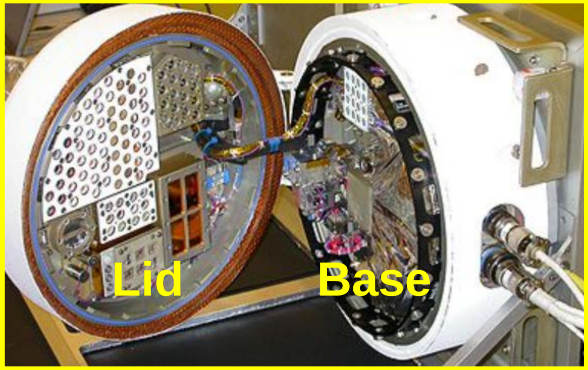

The BIOPAN facilities are installed on the external surface of Foton descent capsules. It has a motor-driven hinged lid, which opens 180° in Earth orbit to expose the experiment samples to the space environment.

Comparison of data between R3DE instrument outside ISS (0.3 g cm^{-2} shielding) and Liulin-ISS inside Russian segment (>20 g cm^{-2} shielding)

3.95-2.7110.7 =1.24 μGy h^{-1}

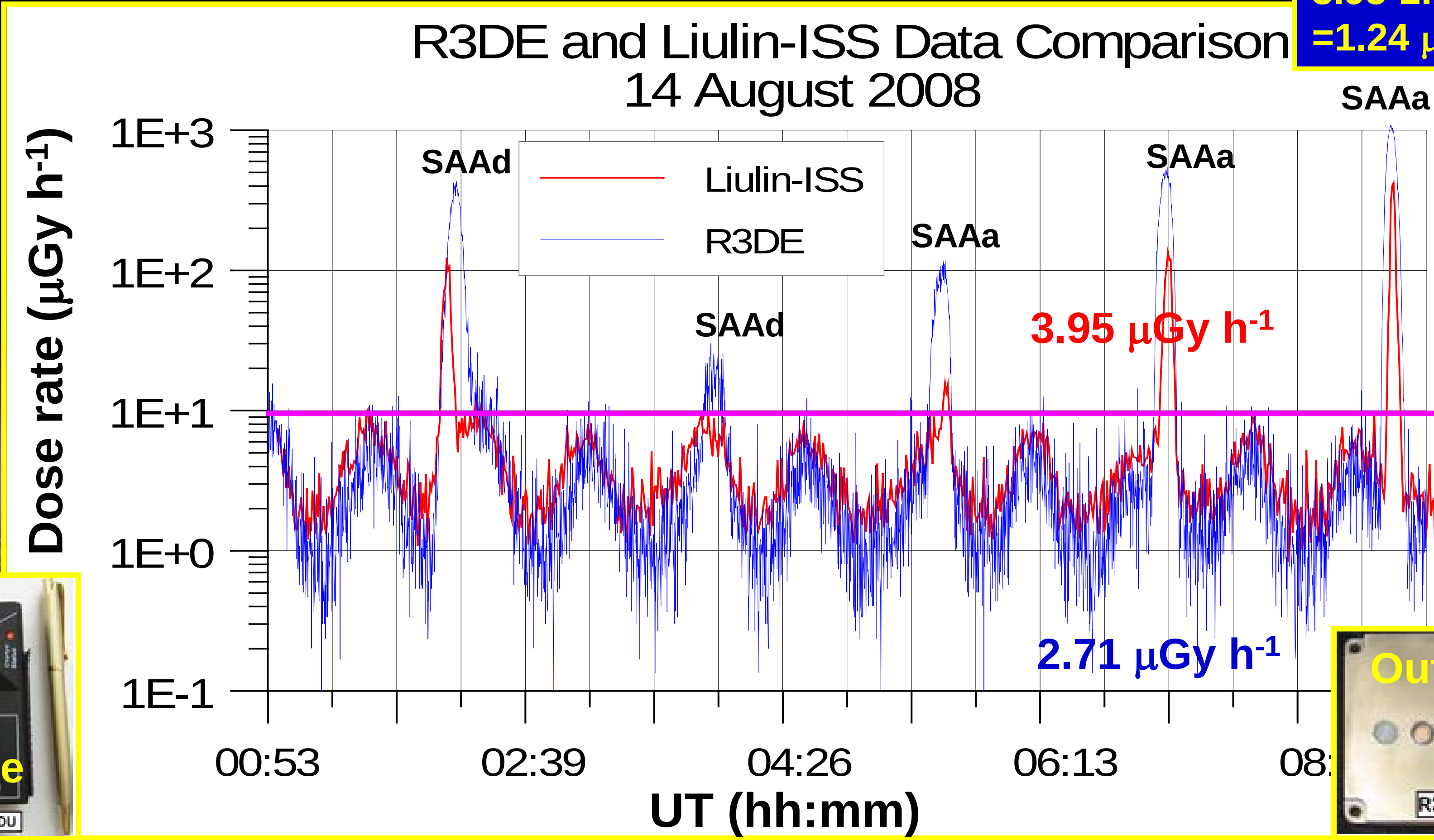

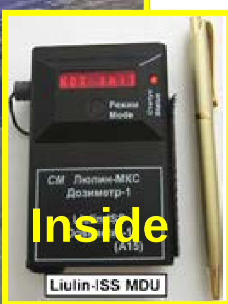

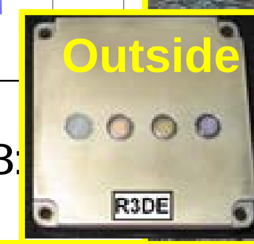

$GCR_{R3DE\ (out)}$	D<10 μGy h^{-1}	Aver. = 2.71 μGy h^{-1}	Accum. = 20 μGy
$GCR_{Liul\_ISS\ (in)}$	D<10 μGy h^{-1}	Aver. = 3.95 μGy h^{-1}	Accum. = 29 μGy
$IRB_{R3DE\ (out)}$	D>10 μGy h^{-1}	Aver. = 261 μGy h^{-1}	Accum. = 341 μGy
$IRB_{R3DE\ (in)}$	D>10 μGy h^{-1}	Aver. = 97 μGy h^{-1}	Accum. = 50 μGy

The conclusion from the shielding dependence investigation in 350-620 km range is:

The dose rate values variations in the latitudinal profile for $4<L<6$ are less than 2 μGy h^{-1}, which is less than the observed long term variations of 4-13 μGy h^{-1}.

Long-term variations of the averaged flux and dose rates observed in the L rage between 4 and 6.2 during 14 Liulin-type experiments between 2001 and 2019. The Liulin data are compared with the monthly values of the modulation parameter (red line) from the ground based cosmic ray data*

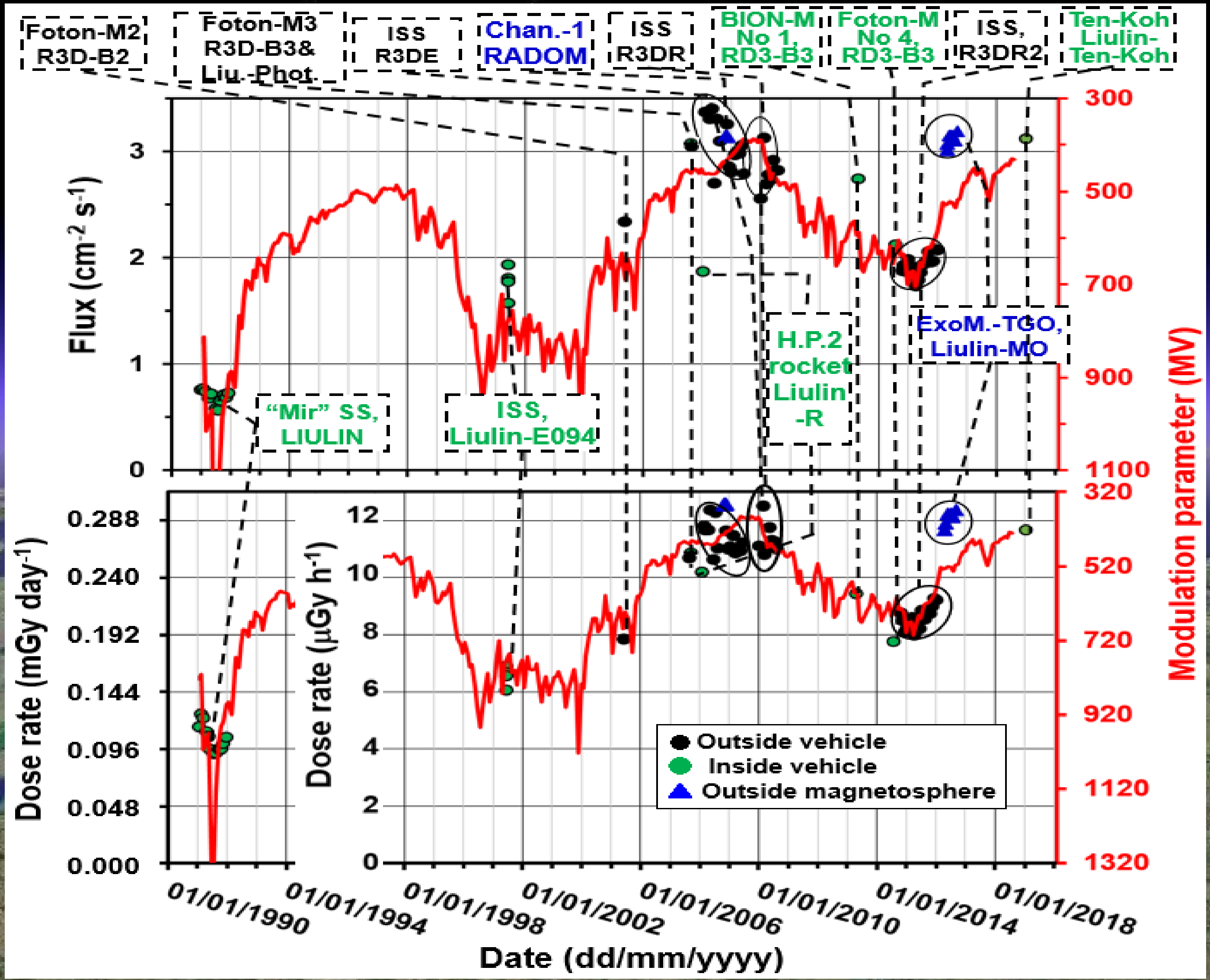

*(Usoskin et al., 2017), http://dx.doi.org/10.1002/2016JA023819

Additional information for the formation of the dose rate values in the previous slide

1. Never the less that different calibration were performed with LIULIN (Dachev et al, 1998) the final coefficient for the transformation of the pulse rate from the VFC to dose rate was overestimated. To match better the LIULIN data with other observations we modify them by subtraction of 5 μGy h^{-1} from the original values. No other instrument values in the picture was modified.

2. The Liulin-MO dose rate data, being obtained from a dosimetric telescope of 2 detectors, to be in accordance with other data takes only the data from the first detector, adjusted exactly in same way as the other single detector data.

3. Never the less that the Liulin-Ten-Koh dose rate data was obtained in 3 months the averaged dose rate is presented with 1 point in January 2019.

Comparison of Liulin GCR dose measurements with other experiments and models

Example of middle range GCR measurements comparison by 2 DOSTEL devices and R3DR2 instrument on ISS

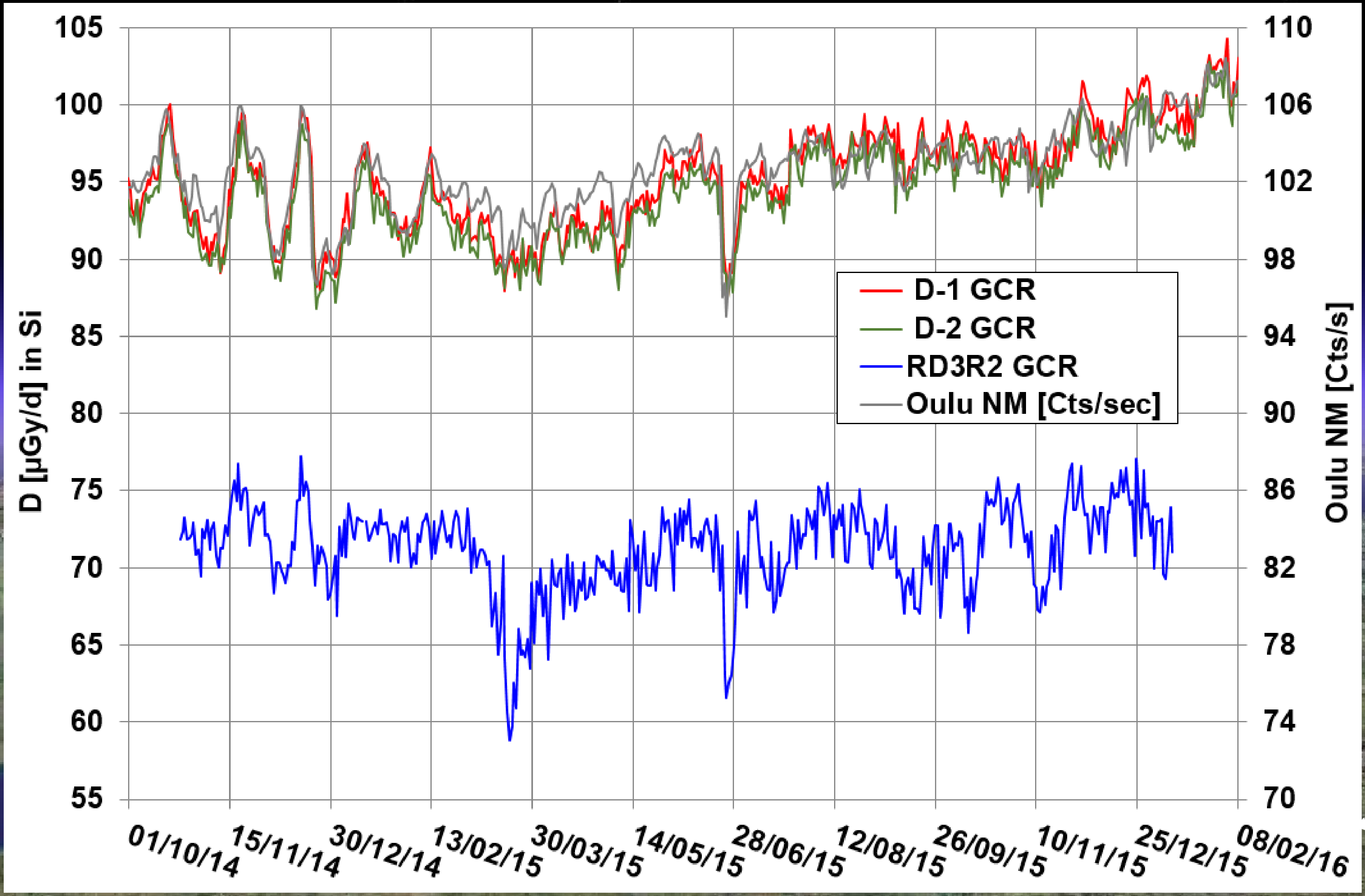

The short term variations of the global GCR dose rate are in good coincidence with the Oulu NM count rate and depends by the Dst index

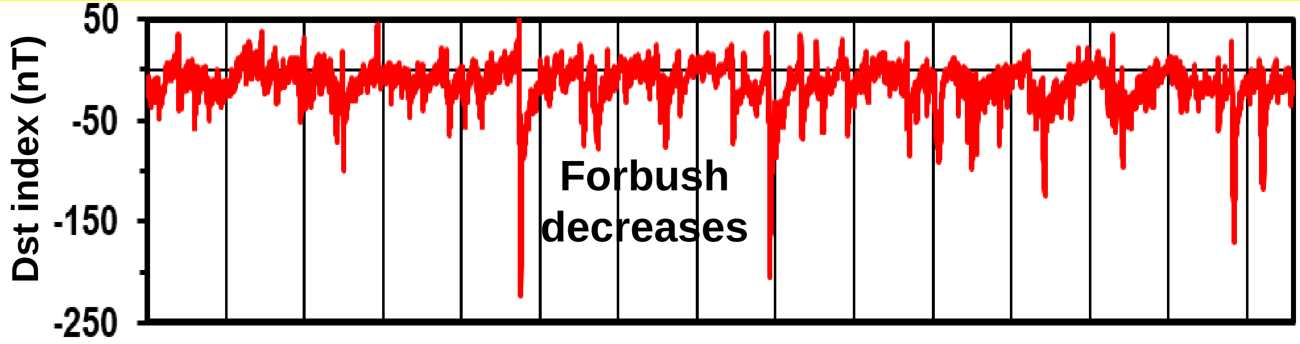

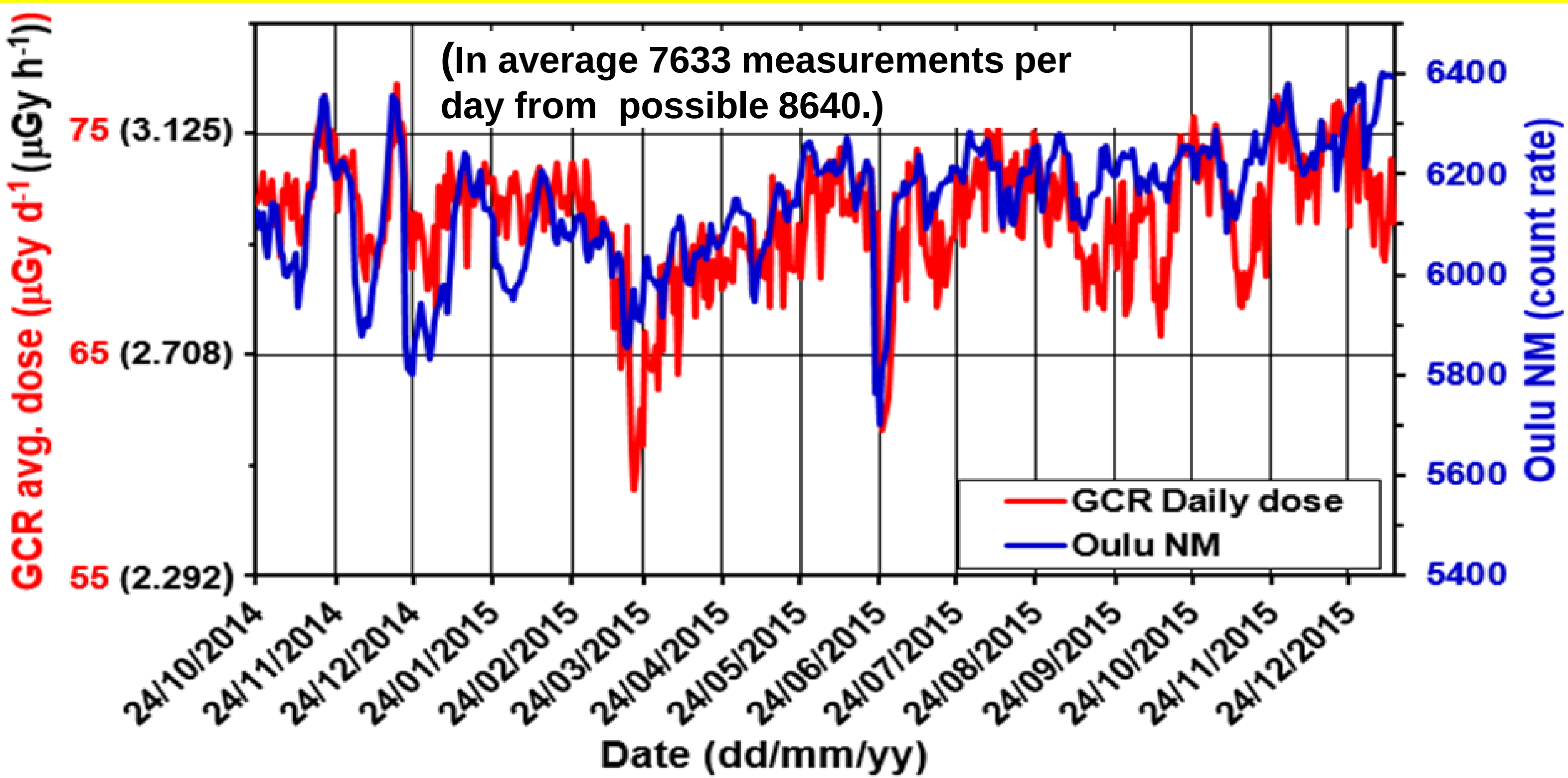

Comparison of measured (m) by Liulin-E094 four MDUs inside American segment of ISS with calculated (c) by NASA HZTRN model average dose rates

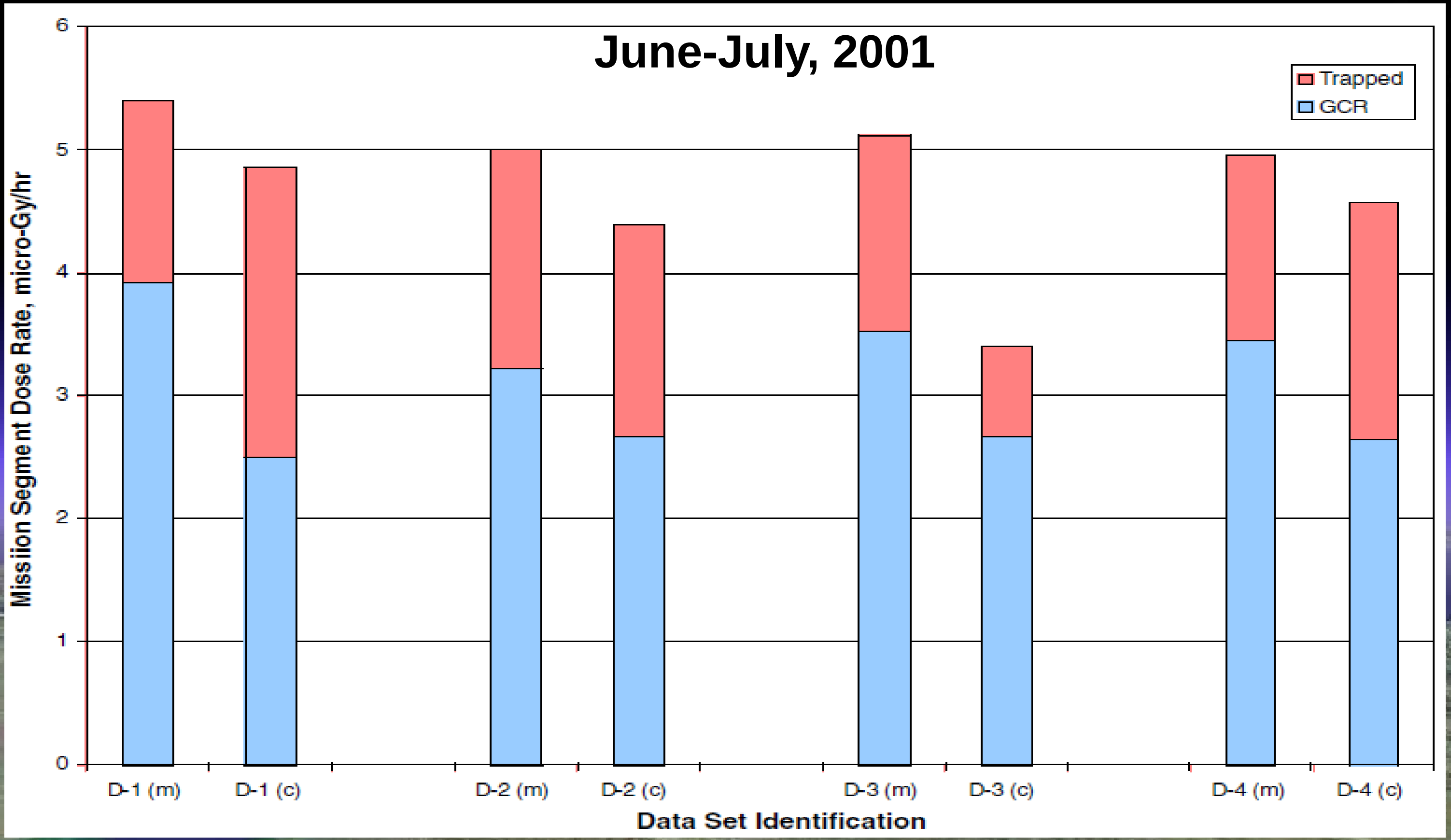

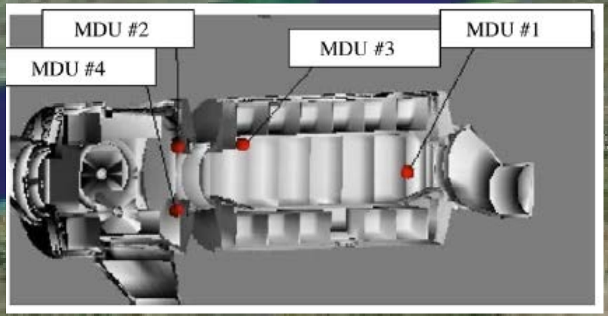

Nealy, J. E., F. A. Cucinotta, J. W. Wilson, F. F. Badavi, N. Zapp, T. Dachev, B.T. Tomov, E. Semones, S. A. Walker, G. de Angelis, S. R. Blattnig, W. Atwell, Pre-engineering spaceflight validation of environmental models and the 2005 HZETRN simulation code, Adv. Space Res., 40, 11, 1593-1610, 2007. http://dx.doi.org/10.1016/j.asr.2006.12.030

Statistical validation of HZETRN as a function of vertical cutoff rigidity using ISS measurements

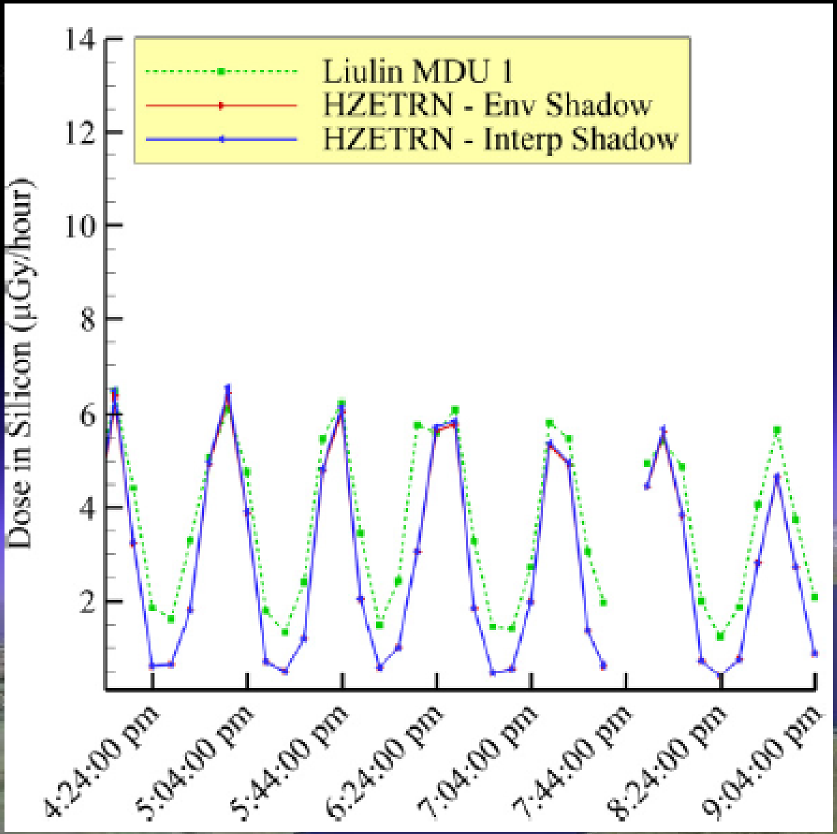

Comparison of binned HZETRN results and Liulin MDU 1 data on ISS from July 6, 2001 4:04 pm to July 6, 2001 9:05 pm. The "Env Shadow" and "Interp Shadow" results are almost identical. Dose is calculated in silicon

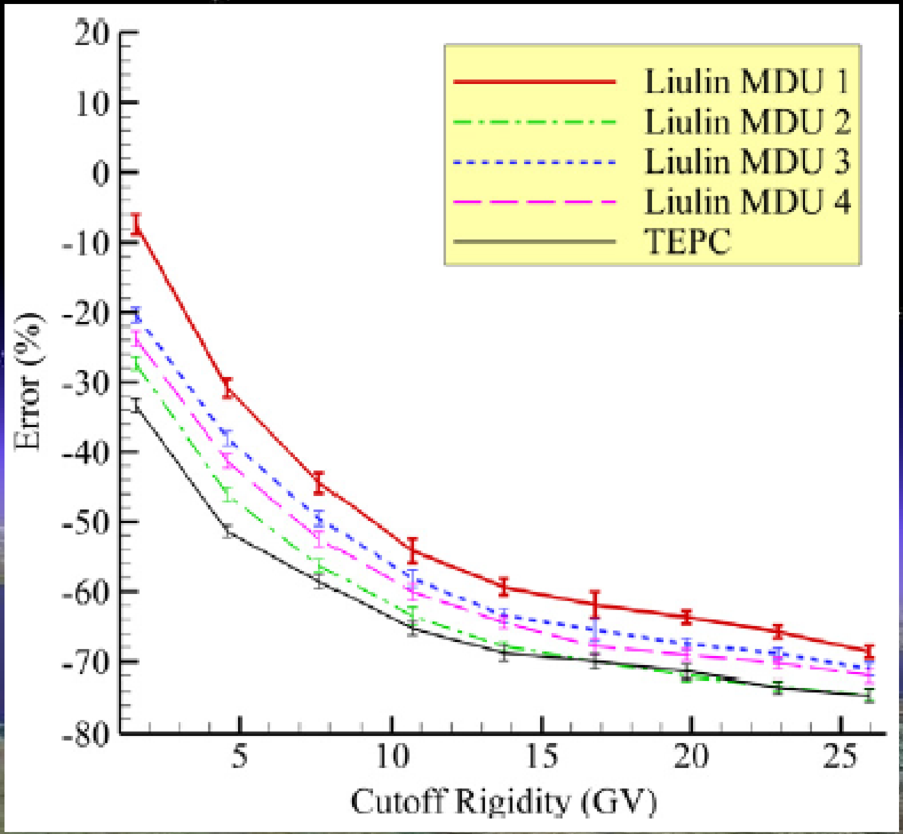

Average errors between HZETRN and the Liulin and TEPC detectors. The error bars represent the 95% confidence interval on the sample mean. Dose is calculated in tissue for the TEPC and silicon for the Liulin detectors

Slaba, T.C., S.R. Blattnig, F.F. Badavi, N.N. Stoffle, R.D. Rutledge, K.T. Lee, E.N. Zappe, T.P. Dachev and B.T. Tomov, Statistical Validation of HZETRN as a Function of Vertical Cutoff Rigidity using ISS Measurements, Adv. Space Res., 47, 600-610, 2011. http://dx.doi.org/10.1016/j.asr.2010.10.021

There is relatively good coincidence between our flux data and the GCR flux data used in the paper by Kuznetsov et al., 2017*

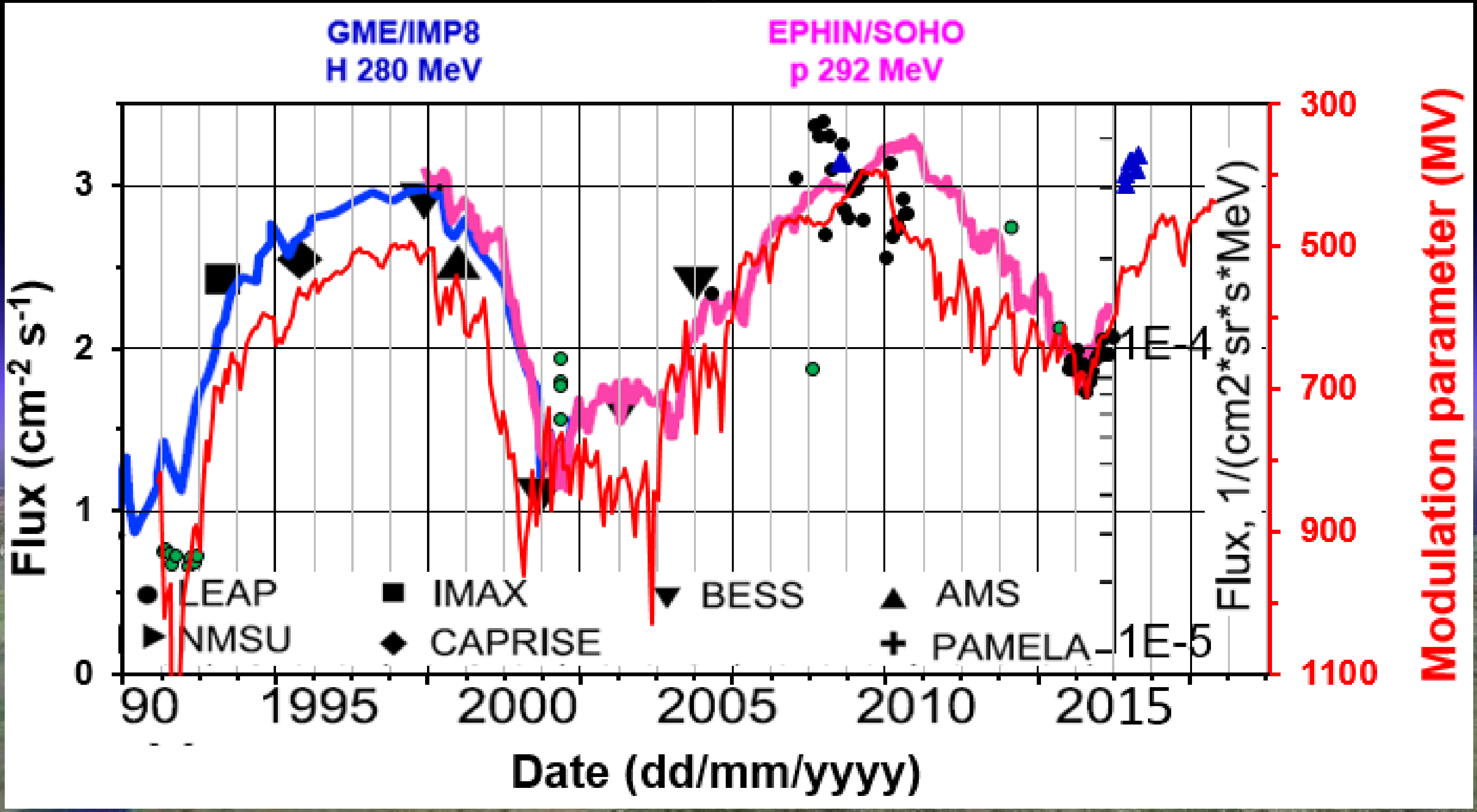

*Kuznetsov, N. V., H. Popova, and M. I. Panasyuk (2017), Empirical model of long-time variations of galactic cosmic ray particle fluxes, J. Geophys. Res. Space Physics, 122, 1463–1472, doi:10.1002/2016JA022920.

Comparison of the measured with Liulin instruments dose rates data with the GCR calculations in free space by Banjac et al., 2019

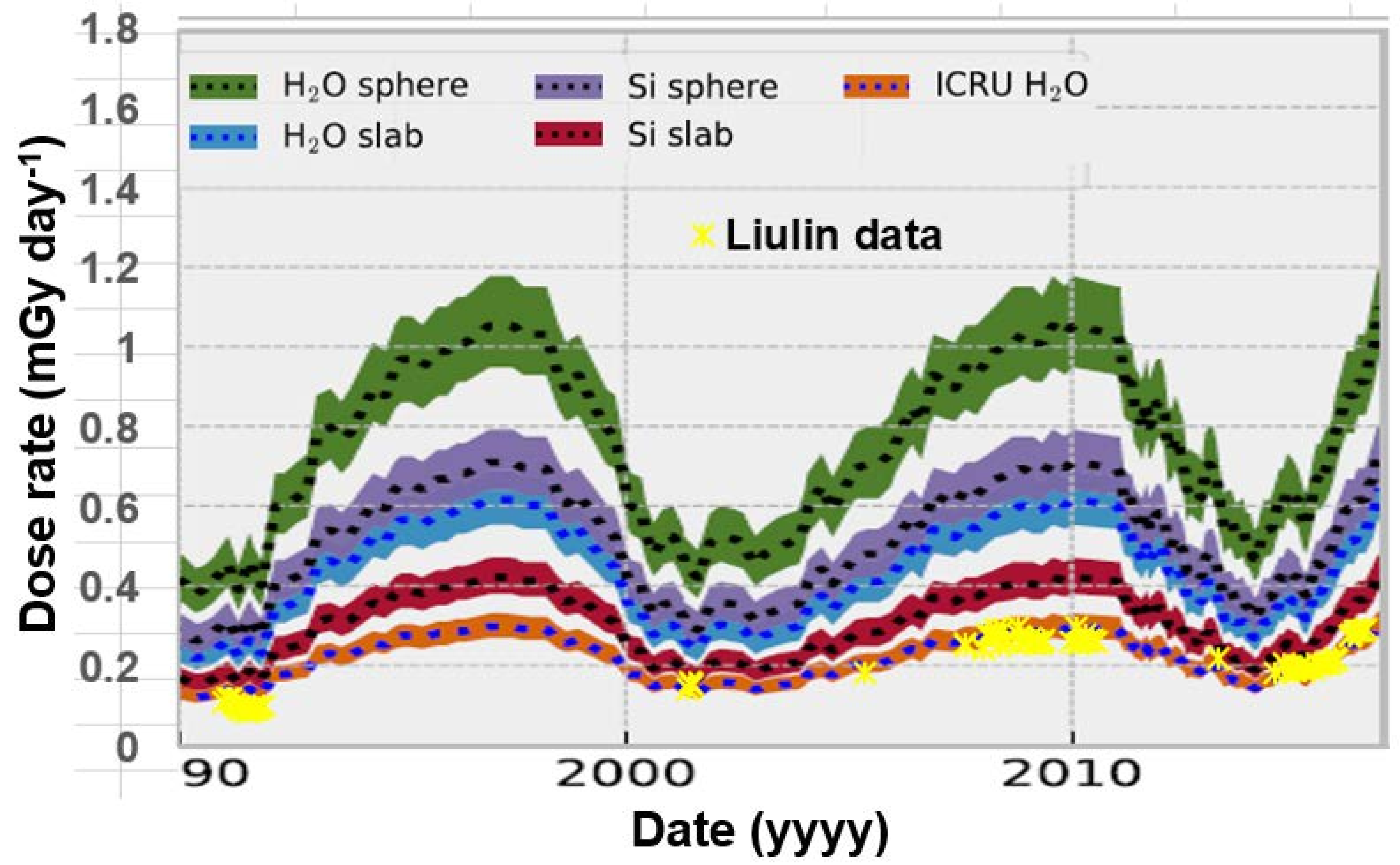

Banjac S, Berger L, Burmeister S, Guo J, Heber B, et al. 2019. Galactic Cosmic Ray induced absorbed dose rate in deep space – Accounting for detector size, shape, material, as well as for the solar modulation. J. Space Weather Space Clim. 9, A14. https://doi.org/10.1051/swsc/2019014

Comparison of the measured with Liulin instruments dose rates data with the GCR calculations for CRaTER shielding by Banjac et al., 2019*

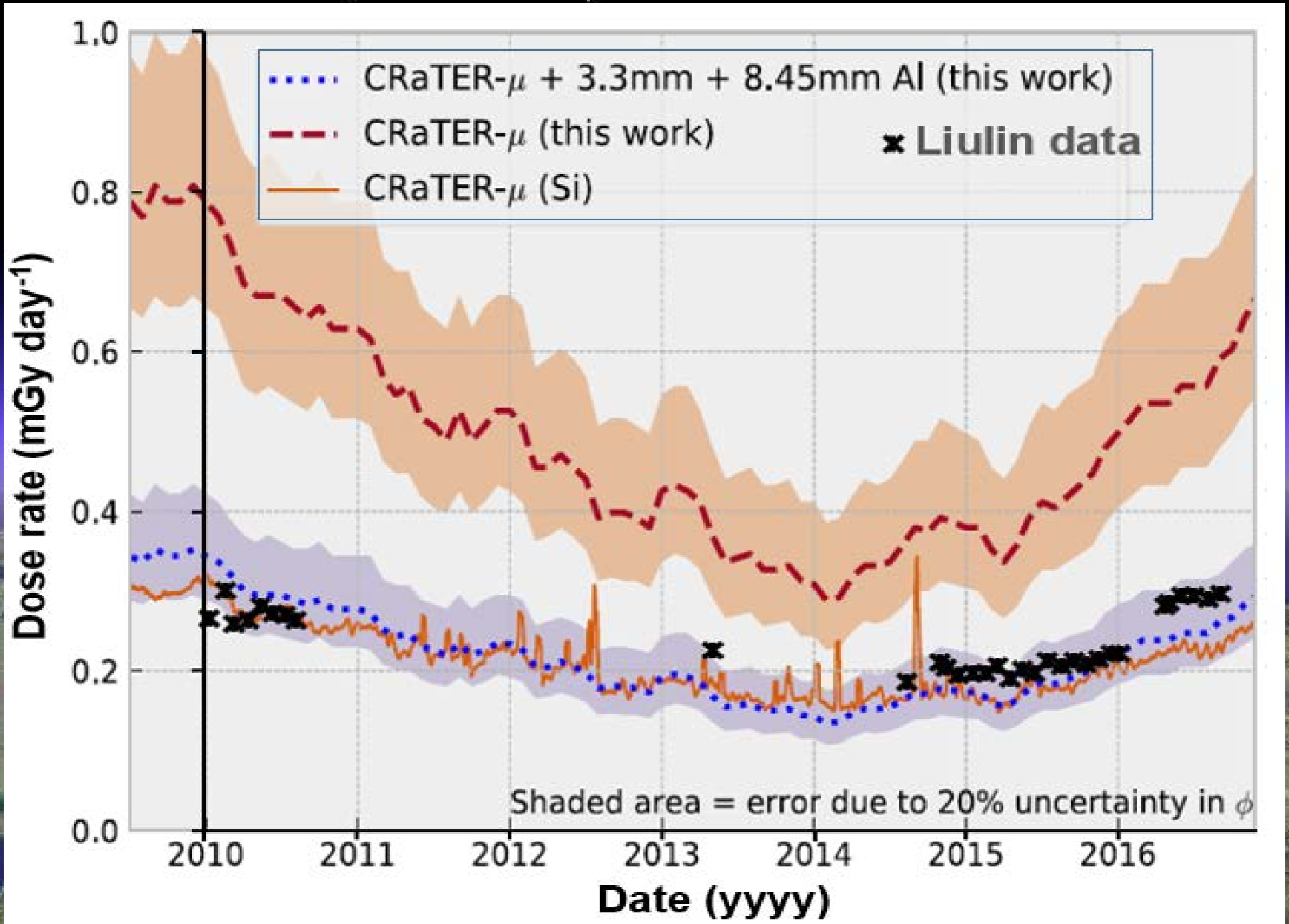

*Banjac S, Berger L, Burmeister S, Guo J, Heber B, et al. 2019. Galactic Cosmic Ray induced absorbed dose rate in deep space – Accounting for detector size, shape, material, as well as for the solar modulation. J. Space Weather Space Clim. 9, A14. https://doi.org/10.1051/swsc/2019014

Conclusions

- The most important achievement of the paper is the proof of the solar modulation of the long-term variations of the averaged flux and dose rates observed in the L range between 4 and 6.2 or outside the magnetosphere during 14 Liulin-type experiments between 2001 and 2019;

- The major advantage of the data is that they are obtained by the electronically identical Liulin type instruments;

- These experimentally obtained data can be used for the modelling of the GCR space radiation risks to the humans in the near Earth radiation environment.

Acknowledgements and data availability

The authors are grateful to G. Horneck, D.P. Häder, and G. Reitz for the overall German–Bulgarian cooperation in the Biopan and EXPOSE projects.

This work was partially supported by Contract No. 4000117692/16/NL/NDe funded by the Government of Bulgaria through an ESA Contract under the Plan for European Cooperating States (PECS).

Most of the dose rate data used in this paper are part of the "Unified web-based database with Liulin-type instruments' cosmic radiation data", which are available online, free of charge at the following URL:

http://esa-pro.space.bas.bg/database

Thank you for your attention*

The L>4 hourly dose rate variations don't coincide so well with the Oulu NM variations probably because the much larger statistics of the globally averaged data (7633 measurements per day from possible 8640). The L>4 statistic is based in average on 901 measurements per day

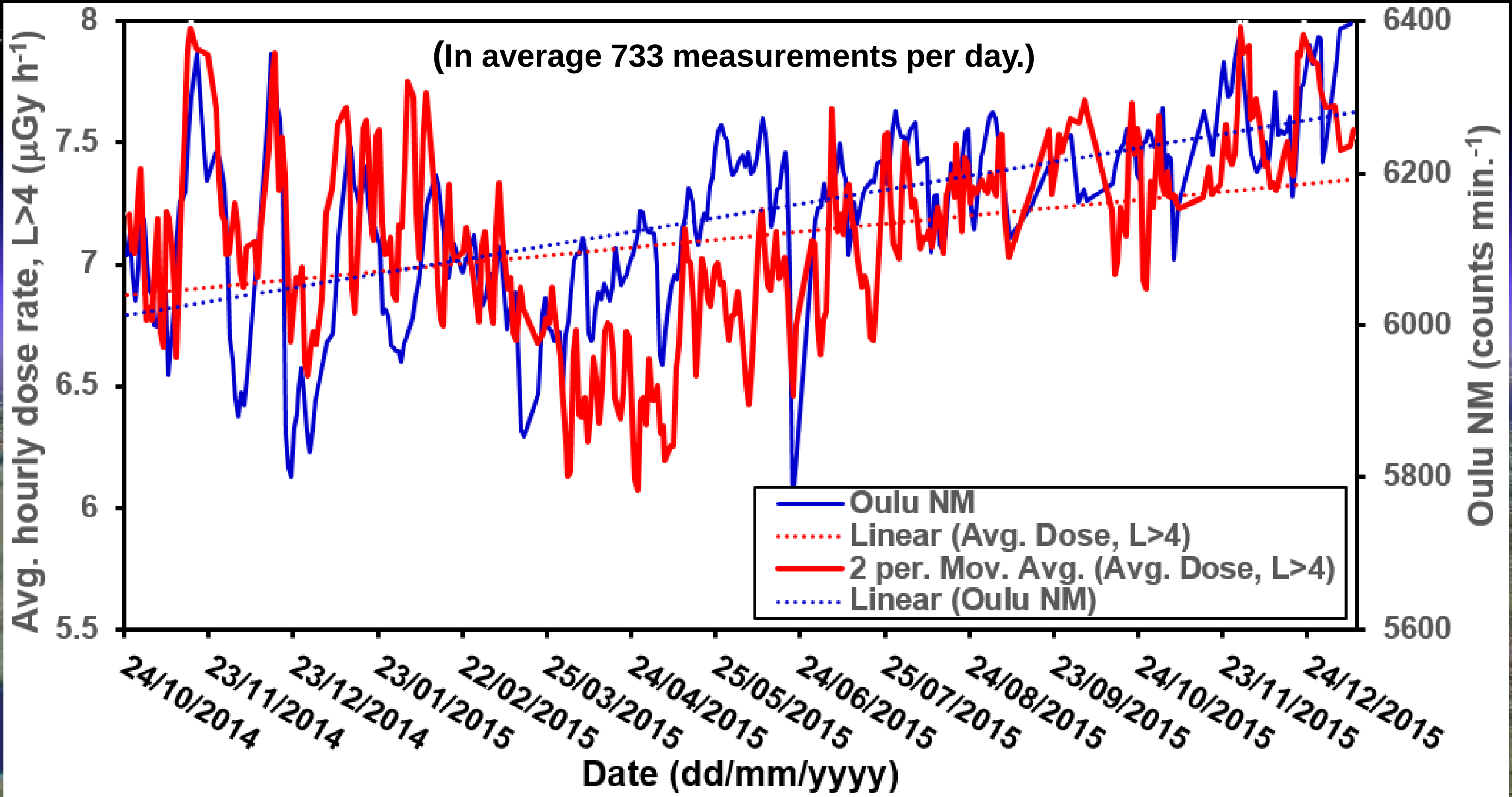

Altitudinal profile up to ~ 90,000 km

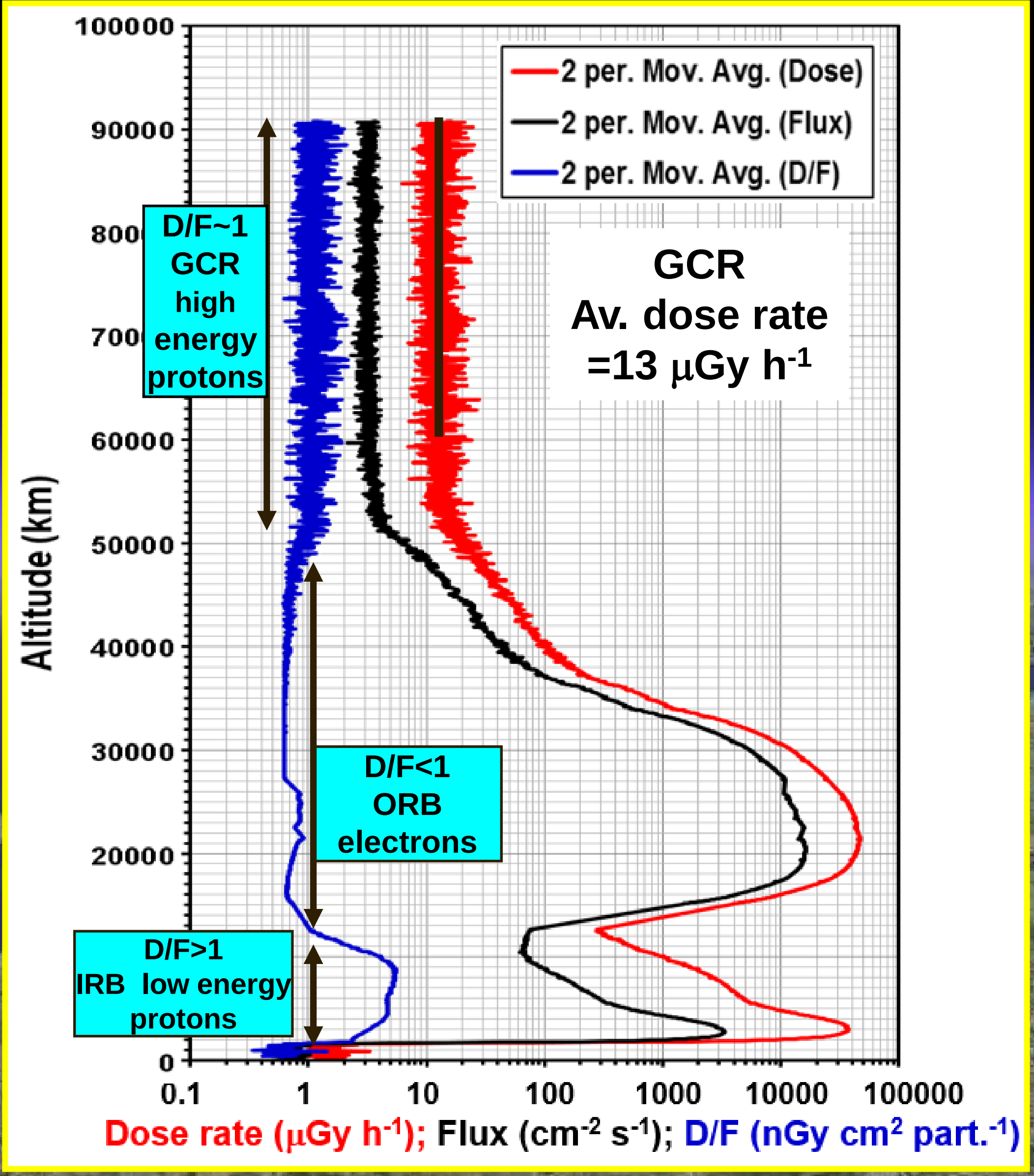

Preliminary outlook of the available GCR dose rate data and range of the dose rate variation between 4 and 13 $\mu Gy\ h^{-1}$